JOURNAL OF VIROLOGY, May 1994, p. 3250–3266
0022-538X/94/$04.00+0

Vol. 68, No. 5

Mapping of Intracellular Localization Domains and Evidence for Colocalization Interactions between the IE110 and IE175 Nuclear Transactivator Proteins of Herpes Simplex Virus

MARY-ANN MULLEN,[1]† DOLORES M. CIUFO,[2] AND GARY S. HAYWARD[1,2]*

The Virology Laboratories, Department of Pharmacology and Molecular Sciences,[1] and Department of Oncology,[2] Johns Hopkins University School of Medicine, Baltimore, Maryland 21205

Received 15 November 1993/Accepted 31 January 1994

Transcriptional regulation by the IE175 (ICP4) and IE110 (ICP0) phosphorylated nuclear proteins encoded by herpes simplex virus (HSV) appears to be a key determinant for the establishment of successful lytic cycle infection. By indirect immunofluorescence in transient DNA transfection assays, we have examined the intracellular distribution of deletion and truncation mutants of both IE175 and IE110 from HSV-1. Insertion of short oligonucleotides encoding the basic amino acid motifs 726-GRKRKSP-732 from IE175 and 500-VRPRKRR-506 from IE110 into deleted cytoplasmic forms of the two proteins restored the karyophilic phenotype and confirmed that these motifs are both necessary and sufficient for proper nuclear localization. Analysis of IE110 deletion mutants and a panel of IE110/IE175 hybrid proteins was also used to evaluate the characteristic IE110 distribution within nuclear punctate granules as seen by immunofluorescence and phase-contrast microscopy. The phase-dense punctate pattern persisted with both large C-terminal truncations and deletions of the Cys-rich zinc finger region and even with a form of IE110 that localized in the cytoplasm, implying that the punctate characteristic is an intrinsic property of the N-terminal segment of the IE110 protein. Transfer of the full IE110-like punctate phenotype to the normally uniform diffuse nuclear pattern of the IE175 protein by exchange of the N-terminal domains of the two proteins demonstrated that the first 105 to 244 amino acids of IE110 represent the most important region for conferring punctate characteristics. Surprisingly, cotransfection of a wild-type nuclear IE175 gene together with the IE110 gene revealed that much of the IE175 protein produced was redistributed into a punctate pattern that colocalized with the IE110-associated punctate granules seen in the same cells. This colocalization did not occur after cotransfection of IE110 with the IE72 (IE1) nuclear protein of human cytomegalovirus and therefore cannot represent simple nonspecific trapping. Evidently, the punctate phenotype of IE110 represents a dominant characteristic that reveals the potential of IE110 and IE175 to physically interact with each other either directly or indirectly within the intracellular environment.

Herpes simplex virus (HSV) initiates lytic cycle infection in a wide variety of host cell types in culture. However, in vivo it also establishes quiescent latent state infections in both human and animal hosts in sensory neurons. Two virus-encoded regulatory genes known as IE175 (or ICP4) and IE63 (or ICP27) that are synthesized under immediate-early (IE) conditions (reviewed in reference 26) are essential for progression of the full lytic cycle gene expression cascade in cell culture conditions (12, 50). The IE175 protein behaves as a specific transcriptional transactivator of downstream delayed-early and late viral promoters in both virus-infected and DNA-transfected cells (12, 14, 21, 38, 41, 46, 54), whereas the IE63 protein appears to act primarily as a posttranscriptional regulator of late viral gene expression. IE175 is also a specific DNA-binding protein that binds to DNA target sites near the transcription initiation site of several viral promoters, including its own, to produce a down-regulation phenotype (19, 37, 39, 48).

Two other HSV-encoded regulatory genes act as accessory transcriptional transactivators (reviewed in reference 26). During initial infection by virions, the VP16 (VF65 or αTIF) structural protein introduced with the input virus particles positively regulates all of the IE class transcripts by forming activated complexes with the cellular Oct-1 protein bound to overlapping octamer and TAATGARAT sites within the IE response elements of appropriate viral target promoters. However, in the absence of VP16, for example during reactivation from latency (25, 32, 49, 57) and after infection with naked uncoated DNA molecules (4), a third IE class nuclear regulatory protein known as IE110 (or ICP0) provides a key alternative trigger for activation of lytic cycle events (32, 49, 57). Viruses that are mutant or deleted in their diploid IE110 genes do grow in cell culture, but they give reduced plaque size and have deficiencies in certain early and late lytic cycle functions (5, 6, 8, 51, 53).

The protein product encoded by the isolated IE110 gene or cDNA behaves as a nonspecific transactivator of virtually all target promoters tested in transient cotransfection assays (14, 15, 21, 38, 41, 46, 56) and also transactivates target HSV genes when it is introduced and expressed from adenovirus or vaccinia virus vectors (58, 59). However, genetic evidence from infection with temperature-sensitive or deletion mutants of IE175 and IE110 implies that IE110 cannot on its own function to activate delayed-early target promoters in the viral genome, whereas IE175 can do so (12, 23, 54). IE175 does appear to require IE110 to be present before an input HSV infection can activate a susceptible target promoter that is in an integrated chromatin-associated state (3).

* Corresponding author. Mailing address: The Virology Laboratories, Department of Pharmacology and Molecular Sciences, Johns Hopkins University School of Medicine, 725 N. Wolfe St., Baltimore, MD 21205. Phone: (410) 955-8686. Fax: (410) 955-8685.

† Present address: Medical College of Wisconsin, Milwaukee, WI 53226.

IE110 differs from IE175 by localizing in characteristic phase-dense intranuclear punctate granules in DNA-transfected cells (11, 17, 22, 23, 30) and in virus-infected cells that are blocked at early stages (29, 30), whereas IE175 on its own displays a uniform diffuse intranuclear pattern that is not phase dense (11, 22, 24, 29, 30, 35, 42). Knipe et al. (29, 30) reported that IE175 and IE110 could sometimes be found to colocalize in infected cells and that an IE175 mutant protein that failed to accumulate in the nucleus blocked entry of the wild-type IE110 protein into the nuclei of infected cells. Gelman and Silverstein (22) further suggested that IE175 could sometimes alter the intracellular distribution of IE110 in DNA-transfected HeLa cells. The possibility of interaction between IE175 and IE110 has also been implied from synergism and altered target specificity effects observed in transient chloramphenicol acetyltransferase expression assays when the two were cotransfected (9, 15, 16, 17, 22, 38, 39, 40, 57a). Both IE175 and IE110 have been reported to be selectively associated with virus particles (55), but unlike VP16, they are not major structural components of HSV virions.

Little is known about the mechanisms of promoter targeting during transactivation by either IE175 or IE110, except that the conserved DNA binding domain of the 1,298-amino-acid IE175 protein is important and that the novel RING class zinc finger motifs (20, 43) in the 775-amino-acid IE110 protein are critical. IE175 is a phosphorylated nuclear protein that forms dimers both in solution and when bound to DNA (19, 34). IE110 is also a phosphorylated protein that forms dimers and perhaps multimers in solution (7, 10, 18), but it is not known to bind to DNA specifically.

Several previous reports of functional analysis with deletion or insertion mutations across the IE175 and IE110 proteins included evaluations of their intracellular distribution patterns. The results of those studies mapped the nuclear localization signal (NLS) to within an 80- to 90-amino-acid block near the center of each protein (9, 12, 13, 16, 42) and implied that a C-terminal domain of IE110 confers the punctate characteristics (9, 17). In the present studies, we have used transient DNA transfection and indirect immunofluorescence assays (IFA) with deleted or truncated proteins and a set of IE175/IE110 hybrid proteins to further investigate these characteristics. The results precisely identified a short six- to seven-amino-acid basic motif in each protein that specifies intranuclear localization and led to a reevaluation of the map location of the domains of IE110 associated with the punctate characteristics. We have also detected an apparently specific intracellular interaction between the two proteins that leads to colocalization within punctate granules when they are both introduced into the same DNA-transfected Vero cells.

(These studies represented part of the Ph.D. thesis of M.-A. Harrigan-Mullen [24].)

MATERIALS AND METHODS

Expression plasmids. The p*Xho*I-C effector plasmid containing the intact IE175 gene from HSV-1(KOS) under the control of its own promoter within a 9.5-kb viral DNA fragment was described previously (21, 38, 44). The simian cytomegalovirus (SCMV)/IE175 gene in effector plasmid pGH114, which contains a 5.3-kb *Sal*I-*Dra*I fragment derived from p*Xho*I-C, was also described previously (48). It encodes the intact IE175(1–1298) coding region plus untranslated 5′ leader sequences downstream of position +178 and all 3′ transcriptional control elements placed behind the SCMV major IE (MIE) IE94(−990/+30) promoter/enhancer region (27) in a pBR322 background. Plasmid pGH114, which lacks the IE175 DNA-binding site responsible for negative autoregulation (48), gives approximately fivefold-higher expression of the IE175 protein than does p*Xho*I-C in transiently transfected cells, as judged by the number and intensity of immunofluorescence-positive cells. The large internally deleted version of IE175(Δ355–833) in pGH115, which was used for nuclear localization assays, was created by deleting between two in-frame *Stu*I sites and inserting a 12-mer *Bgl*II linker oligonucleotide. Similarly, the smaller internally deleted version, IE175(Δ524–574) in pGH118, was produced by rejoining between the two in-frame *Bam*HI sites. The C-terminal truncation mutants IE175(*tm*353) and IE175(*tm*833) in pGH116 and pGH117 and IE175(*tm*1029) in pMM61 and pMM45 were constructed by inserting 14-mer *Xba*I triple terminator oligonucleotides at the second or third *Stu*I site (after partial digestion) and at the single *Hin*cII site in pGH114.

Two different parental versions of intact IE110 expression plasmids were constructed in which the intact HSV-1(KOS) IE110(1–775) coding region was placed either under the transcriptional control of its own HSV-1(KOS) IE110 promoter in effector plasmid pGH92 or under control of the SCMV MIE IE94 promoter/enhancer region in pGH94 (SCMV/IE110). In both cases, the IE110 coding cassette consisted of a 4.1-kb *Bgl*II-to-*Kpn*I fragment derived from pIGA15 (21, 38). The 5′ end of the IE110 coding fragment in pIGA15 was first deleted to +120 by *Bal* 31 digestion followed by addition of a *Bgl*II linker and transfer into a pUC18 background as plasmid pGH85. Secondly, the 3′ end was shortened by removal of a 1.2-kb *Kpn*I fragment by partial digestion and rejoining (pGH91). Third, the 950-bp *Hin*dIII-*Bam*HI IE110(−800/+123) promoter fragment from pGH83 (11) was placed upstream between the *Hin*dIII and *Bgl*II sites to create pGH92. Alternatively, the 1,020-bp *Hin*dIII-*Bgl*II IE94(−990/+30) promoter fragment from pGH70 was placed upstream between the *Hin*dIII and *Bgl*II fragments of pGH91 to yield pGH94. The origin of the human cytomegalovirus (HCMV) MIE expression plasmids pRL45 (IE1 plus IE2) and pMP17 (IE1 only) was described previously (31).

IE110 deletion and truncation mutants. IE110 C-terminal truncation mutants were produced by insertion of 14-bp *Xba*I or *Spe*I triple terminators at the flush-ended or T4 polymerase-blunted *Sna*BI, *Nru*I, *Bcl*I, *Mlu*I, and *Bst*EII sites in pGH92 to give plasmids pMM3(*tm*244), pMM5(*tm*244), pMM2(*tm*312), pMM4(*tm*312), pMM65(*tm*364), pMM74(*tm*519), and pMM73 (*tm*713). Out-of-frame insertions of *Bgl*II linkers at blunted *Bcl*I or *Sal*I sites yielded frameshift mutants IE110(*fs*364) in pMM56 and IE110(*fs*768) in pMM82, respectively. A set of seven internally deleted versions of IE110 were constructed either by (i) partial deletion plus insertion of *Bgl*II in-frame adaptors (e.g., *Xho*I-*Bgl*II-*Sph*I [pMM76], *Xho*I-*Bgl*II-*Pvu*I [pMM72], and *Sph*I-*Bgl*II-*Pvu*I [pMM81]); (ii) insertion of appropriate *Bgl*II linkers at blunt-ended *Xho*I, *Sna*BI, *Nru*I, and *Mlu*I sites followed by joining in frame to other *Bgl*II converted sites or to *Bcl*I (pMM68, pGH215, and pMM63); or (iii) direct in-frame removal of internal *Bss*HII fragments (pMM1). These manipulations generated IE110(Δ106–134) in pMM76, IE110(Δ106–177) in pMM72, and IE110(Δ136–177) in pMM81 derived from the pGH92 background and IE110(Δ106–244) in pMM68, IE110(Δ313–363) in pGH215, IE110(Δ365–517) in pMM63, and IE110(Δ399–460) in pMM1 derived from the pGH94 background.

Panel of hybrid IE110/IE175 and IE175/IE110 proteins. Seven IE175-based expression plasmids in which the N terminus of IE175 was replaced with N-terminal coding sequences from IE110 were constructed. Some were derived directly from the effector plasmids described above. Additional flexibility

was created by inserting 8-, 10-, 12-, or 14-mer symmetrical oligonucleotide pairs containing a central *Bgl*II linker restriction site into the parent wild-type effector plasmids. For example, *Bgl*II linkers were added to IE175 in pGH114 between the first, second, or third *Stu*I site at codons 353, 376, and 835 (pMM12, -13, -19, -27, -28, -30, -31, -34, and -35) and at the *Hin*cII site at codon 1029 (pMM37, -38, and -39). Similarly, one or more *Bgl*II linkers were inserted into IE110 in pGH92 or pGH94 at the *Xho*I (pMM66), *Kpn*I (pMM69), *Sna*BI (pMM17, -18, -42, and -43), *Nru*I (pMM21, -22, -23, -46, -47, and -48), *Mlu*I (pMM64), *Aat*II (pMM77 and -79), and *Bst*EII (pMM70 and -75) sites at codons 105, 212, 244, 312, 518, 553, and 712, respectively. To produce the in-frame hybrid IE110(1–364)/IE175(376–1298) protein in plasmid pGH189, a 5.6-kb *Eco*RI-*Bcl*I fragment from pGH92 was joined to a 3.4-kb *Bcl*I-*Eco*RI fragment from pGH114. The hybrid IE110(1–364)/IE175(834–1298) gene in plasmid pGH199 was formed by fusion of a 5.6-kb *Eco*RI-*Bcl*I fragment from pGH92 to a 2.7-kb *Bgl*II-*Eco*RI fragment from pMM13. Plasmid pGH238 encoding IE110(1–312)/IE175(576–1298) was constructed by moving a 2.8-kb *Hin*dIII-*Bgl*II fragment from pMM21 and a 2.3-kb *Bam*HI-*Xba*I fragment from pGH114 into the pKP54 plasmid vector between the *Hin*dIII and *Xba*I sites. The hybrid IE110(1–244)/IE175(84–1298) gene in plasmid pGH186 was created by fusion of a 5.2-kb *Eco*RI-*Sna*BI fragment from pGH92 with a 4.9-kb *Pvu*II-*Eco*RI fragment from pGH114. To make IE110(1–244)/IE175(834–1298) in the pGH217 expression plasmid, a 5.7-kb *Eco*RI-to-*Bgl*II fragment from pMM17 was ligated together with a 2.7-kb *Bgl*II/*Eco*RI fragment from pMM12. To create plasmid pGH187 containing the IE110(1–244)/IE175(1030–1298) hybrid gene, a 5.2-kb *Eco*RI-*Sna*BI fragment from pGH92 was joined to a 2.1-kb *Hin*cII-*Eco*RI fragment from pGH114. Finally, an IE110(1–105)/IE175(376–1298) hybrid protein gene in plasmid pMM84 was constructed by ligating a 4.7-kb *Eco*RI-*Bgl*II fragment from pMM72 with a 3.6-kb *Bcl*I-*Eco*RI fragment from pGH114.

Three reciprocal IE175/IE110 expression plasmids in which N-terminal fragments from IE175 were exchanged for the N terminus of IE110 were also constructed. Plasmid pGH198 containing an IE175(1–83)/IE110(245–775) hybrid gene was derived by fusion of a 5.2-kb *Eco*RI-partial *Pvu*II fragment from pGH114 in frame to a 2.6-kb *Sna*BI-*Eco*RI fragment from pGH94. Plasmid pGH216 containing an IE175(1–354)/IE110(313–775) hybrid gene was derived by joining a 5.5-kb *Eco*RI-*Bgl*II fragment from pMM12 to a 2.3-kb *Bgl*II-*Eco*RI fragment from pMM48. Plasmid pGH190 containing an IE175(1–523)/IE110(364–775) hybrid gene was constructed by ligating a 6.5-kb *Eco*RI-*Bam*HI fragment from pGH114 to a 2.1-kb *Bcl*I-*Eco*RI fragment from pGH92.

NLS motifs. Assays for identification of potential NLSs were carried out by DNA transfection followed by IFA. Input test plasmid DNA clones contained in-frame insertions of annealed pairs of complementary synthetic oligonucleotides added at internal *Bgl*II sites within deleted IE175 (pGH115) or IE110 (pMM63) effector plasmids that express cytoplasmic forms of the two proteins. The following oligonucleotide pairs were used in these studies: LGH52/53 (HSV-1 IE175 NLS motif) (5′-GATCGGGCGCAAGCGCAAGAGTCCCGA-3′ and 5′-GATCTCGGGACTCTTGCGCTTGCGCCC-3′), LGH155/157 (HSV-1 IE110 NLS motif) (5′-GATCGTGC GTCCGAGGAAGAGGCGCCA-3′ and 5′-GATCTGGCGC CTCTTCCTCGGACGCAC-3′), LGH226/227 (IE175) (5′-GATCCCGCCGCGGAGACGTCGTCACCA-3′ and 5′-GA TCTGGTGACGACGTCTCCGCGGCGG-3′), and LGH269/270 (Epstein-Barr virus [EBV] Zta) (5′-GATCCCGGCAC GACGCACACGGAAACCACA-3′ and 5′-GATCTGTGGT TTCCGTGTGCGTCGTGCCGG-3′).

The LGH52/53 pair encoding IE175 codons 726-(I) GRKRKSP(EI)-732 was added in both orientations to cytoplasmic IE175(Δ355–833) in pGH115 to produce plasmids pMM6a and pMM6b. Similarly, the LGH155/157 pair encoding IE110 codons 500-(I)VRPRKRR(QI)-506 was added to pGH115 to produce pMM8a and pMM8b and to cytoplasmic IE110(Δ365–517) in pGH63 as 500-(S)VRPRKRR(R)-506 to produce pMM85a and pMM85b. The LGH226/227 pair encoding IE175 164-(I)PPRRRRH(QI)-170 was added to pGH115 to produce pMM20a and pMM20b, and LGH269/270 encoding EBV Zta amino acids 152-(I)PARRTRKP(QI)-157 was added to pGH115 to produce pMM14a and pMM14b.

Monoclonal and antipeptide antibodies. The following peptides from near the N terminus of both proteins were synthesized at the Johns Hopkins Medical School Peptide Facility and shown to be greater than 90% pure by high-pressure liquid chromatography characteristics: IE175(N) (2-EPRPGASTRR PEGRPQRE-19) and IE110(N) (3-SENLQRPGSPGPTDGP PPT-21). A D-Tyr was added to the N terminus and Ser-Cys was added to the C terminus, and the peptides were conjugated to keyhole limpet hemocyanin and used as immunogens in rabbits as described previously by Pizzorno et al. (45). An IE110 C-terminus-specific polyclonal antipeptide antibody (PAb) was generated in a similar fashion (10). Mouse 58S anti-IE175 monoclonal antibody (MAb) (52) was prepared from clarified ascites fluid. Mouse H1083 anti-IE110 MAb ascites fluid was obtained from Lenore Pereira (1). Mouse MAb 810 against HCMV IE1 was obtained from Chemicon International Inc. (El Segundo, Calif.).

Transient DNA transfection and IFA. Short-term DNA transfection of CsCl-purified plasmid DNA by the calcium phosphate-plus-glycerol shock procedure in *N*-2-hydroxyethylpiperazine-*N*′-2-ethanesulfonic acid (HEPES) or BBS buffer (16) was carried out in Vero or 293 cell monolayers, using 2 μg of DNA in each two-well slide chamber or 1 μg of DNA in each four-well slide chamber as described by Middleton et al. (35) and LaFemina et al. (31). At 44 h after DNA transfection, the cells were washed in Tris-saline, fixed with absolute methanol (at −20°C), and then incubated with polyclonal antisera at 1:350-fold dilution in Tris-saline followed by fluorescein isothiocyanate (FITC)-labeled goat anti-rabbit immunoglobulin G (IgG) antibody at 1:100-fold dilution. The monoclonal antibodies were used at 1:50 or 1:100 dilution together with FITC-labeled goat anti-mouse IgG. Slides were screened and photographed with a 40× oil immersion objective on a Leitz Dialux 20EB epifluorescence microscope, using Kodak T-Max P3200 or Kodak Technical Pan film and appropriate FITC filter.

Western blotting (immunoblotting). Cultures of 293 cells in 100-mm-diameter dishes were transfected with 12 μg of plasmid DNA and harvested after 48 h. Scraped cells were washed in cold phosphate-buffered saline (PBS), then lysed in 40 mM Tris-HCl (pH 7.4)–150 mM NaCl–1% Nonidet P-40 containing 3 mM phenylmethylsulfonyl fluoride on ice for 10 min, and solubilized by boiling in 0.1 M Tris (pH 7.0)–4% sodium dodecyl sulfate (SDS)–20% β-mercaptoethanol–10% glycerol. Equal amounts of whole-cell extract protein as judged by silver or Coomassie blue staining were loaded on an SDS–7.5% polyacrylamide gel. Proteins were electrophoretically transferred onto nitrocellulose in 20 mM Tris-HCl (pH 8.3)–150 mM glycine–20% methanol–0.1% SDS at 100 mA for 12 h. The filters were blocked by immersion in PBS (0.9% NaCl, 10 mM sodium phosphate [pH 7.2]) with 5% Carnation instant nonfat dried milk overnight at 4°C. Incubation with monospecific

rabbit PAb at 1:1,000-fold dilution was carried out in 5% dried milk–0.3% Tween 20–1× PBS at 4°C for 1 h. After three 20-min washes, alkaline phosphatase-conjugated or horseradish peroxidase (HRP)-conjugated goat anti-rabbit IgG (Bio-Rad) at 1:3,000 dilution was added for 1 h at 4°C followed by thorough washing. Proteins were visualized with the 5-bromo-4-chloro-3-indolylphosphate–nitroblue tetrazolium color development procedure (alkaline phosphatase) or with the enhanced chemiluminescence (ECL) system (Amersham RPN2106), using Kodak XAR film (HRP).

RESULTS

Intracellular distribution of HSV IE175 and IE110 in DNA-transfected Vero cells. Both IE175 and IE110 can be expressed efficiently from their own promoters in DNA-transfected cells, as detected by IFA and functional analysis (14, 17, 21, 30, 35, 38, 46). However, the nuclear distribution patterns of the wild-type IE175 and IE110 proteins are dramatically different (9, 11, 17, 22, 23, 29). We define the pattern shown by the intact wild-type IE175 protein in Vero cells as diffuse and uniform nuclear (Fig. 1a), although at high magnification it also often showed a fine grainy texture. In contrast, for IE110, the pattern primarily consisted of several dozen discrete crisply defined spherical granules in the nucleus that are described as being punctate (Fig. 2a and b). In both cases, staining was usually excluded from the nucleoli. For IE110, most of the medium-size and large punctate structures also corresponded precisely to dense granules that could be seen in the nuclei of IFA-positive cells by phase-contrast microscopy (30) (see Fig. 8a and b). We usually observed between 1 and 3% positive nuclei at 48 h after transfection of Vero cells with plasmids encoding IE175 and IE110 driven by their natural promoters, whereas the use of SCMV enhancer-driven versions boosted these numbers to between 4 and 10% in Vero cells and up to 30% in 293 cells. Two previously described MAbs, namely, 58S for IE175 (52) and H1083 for IE110 (1), were used initially in these studies, and we also prepared rabbit monospecific PAbs against defined synthetic peptides representing the extreme N termini of both proteins for use in IFA and Western blotting.

Confirmation of the structures and stability of deletion proteins. Previous reports have mapped the epitope for 58S to between codons 1134 and 1195 or codons 1270 and 1298 in the HSV-1 IE175 protein (42, 57) and the epitope for H1083 to between codons 400 and 448 in the HSV-1 IE110 protein (57). Our panels of deleted or truncated IE175 and IE110 effector constructions were examined by IFA in transient expression assays in Vero cells. The predicted structures of all of these constructions and the epitope mapping data are summarized in Fig. 3A for IE175 and Fig. 3B for IE110. These results were consistent with the predictions and confirmed that the 58S mouse MAb epitope mapped between codons 1030 and 1298 in IE175 and that the IE110 H1083 MAb epitope mapped between codons 398 and 461 in IE110. In both cases, the validity of the constructions that failed to react with the MAbs was confirmed by IFA with the N-terminal antipeptide antisera. Similarly, the two rabbit PAbs mapped to their expected locations at the N terminus of each protein, and none of the four antibody preparations gave any cross-reactions with the noncognate effector plasmid. In general, the frequencies and intensities of positive IFA signals were equivalent with all constructions tested. However, for both proteins, the smallest N-terminal fragments tested failed to react with either type of antibody, even in 293 cells, suggesting either that the IE175(1–353) and IE110(1–244) genes encode unstable polypeptides or that these products were synthesized but then lost during methanol fixation. The efficiency of expression of IE110(1–312) was also decreased, as judged by the lower intensity of the IFA signal and a greatly reduced number of positive cells.

The validity of our various deletion and truncation constructions and evaluation of the stability of the proteins produced was also addressed by Western blotting after short-term DNA transfection into 293 cells. Whole-cell extracts were fractionated on SDS-polyacrylamide gels and reacted with the N-terminal peptide antibodies for IE175 (Fig. 4A) and for IE110 (Fig. 4B). In all cases, the products were predominantly intact and generally compatible with the anticipated sizes, taking into account the anomalously high apparent molecular weights of both parent wild-type proteins in SDS-gels (although several gave doublet bands). Once again, the products of IE175(1–353) (Fig. 4A, lane 4) and IE110(1–244) (not shown) were undetectable, implying that they were indeed unstable, although the IE110(1–312) protein was present at approximately 10% of the relative abundance of the other forms of IE110 (Fig. 4B, lanes 10 and 11).

Deletion of the NLS domains. In contrast to the wild-type IE175 protein, the internally deleted IE175(Δ355–833) product was localized virtually exclusively in the cytoplasm by IFA (Fig. 1b). However, four other deleted forms of IE175 that were tested, including IE175(*tm*833) (Fig. 1c), all displayed the usual nuclear diffuse distribution pattern (summarized in Fig. 3A). The measured ratios of exclusively nuclear to exclusively cytoplasmic distribution (N/C ratios) for all IE175 constructions tested are listed in Table 1, experiment 1. Previous results from other groups have placed a critical domain specifying nuclear localization for IE175 more precisely between codons 591 and 773 (12, 13) or between codons 682 and 774 (42).

Deletion between codons 364 and 519 in IE110 produced an exclusively cytoplasmic product (Fig. 2c and d). In contrast, after deletion of codons 399 to 460, the IE110 product was still nuclear (Fig. 5d). Truncation at codon 519 or 713 and all deletions tested within exon 2 or in the front portion of exon 3 also gave exclusively nuclear products (Fig. 5a to c and h), whereas truncation or frameshifts at 312 or 364 gave mixed nuclear and cytoplasmic products (Fig. 5e to g). The measured N/C ratios for some of these examples are listed in Table 2, experiment 1. These results, which are summarized in Fig. 3B, confirmed that the most prominent signal for stable nuclear localization for IE110 must map either between codons 365 and 398 or between codons 461 and 518. The latter location is consistent with previous work by Everett (17), who found that a region between codons 475 and 540 was required for nuclear localization of IE110.

Restoration of nuclear localization by insertion of the putative NLS motifs. In both proteins, proposed NLSs of the clustered basic amino acid motif type containing Lys, Arg, and Pro residues are evident within the appropriate deleted region (13, 42). To determine whether these predicted motifs, which are similar to that found in simian virus 40 large T antigen (28), were necessary and sufficient, we inserted oligonucleotides encoding the putative NLS motifs in frame back into a *Bgl*II linker site in the cytoplasmic IE175(Δ355–833) deletion construction. A number of possible basic motifs from IE175, IE110, and other sources were tested in both forward and inverted orientations. The results shown in Table 1, experiment 2, include data pooled from two or three separate experiments with between 200 and 400 positive cells scored for each of several independent clones. Cells with mixed nuclear and cytoplasmic staining were recorded in a separate category from those that were exclusively nuclear or exclusively cytoplasmic. For comparison, the intact IE175(1–1298) protein, the IE175(Δ524–574) deletion, and the IE175(*tm*833) and

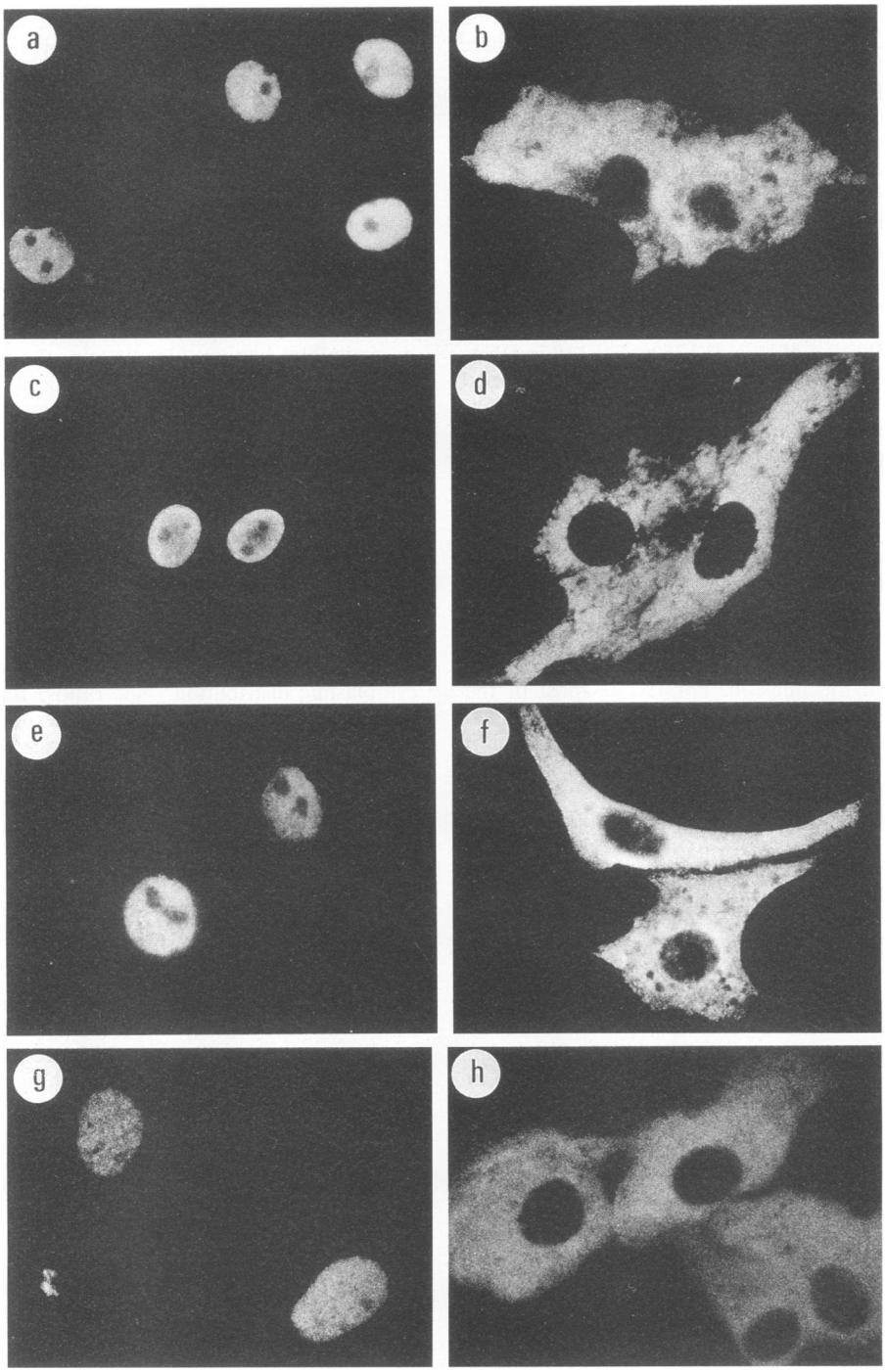

FIG. 1. Intracellular localization patterns of IE175 protein variants after transient expression in DNA-transfected Vero cells and identification of an NLS in IE175. The photomicrographs show methanol-fixed cells after detection by IFA with IE175-specific antibodies. (a) Wild-type nuclear diffuse IE175(1–1298) encoded by plasmid pGH114; (b) cytoplasmic diffuse IE175(Δ355–833) encoded by the pGH115 deletion variant; (c) nuclear diffuse IE175(*tm*833) from pGH117; (d) cytoplasmic test vector IE175(Δ355–833) containing the inserted LGH226/227 oligonucleotide pair encoding IE175 164-PPRRRRH-170 (pMM20a); (e and f) IE175(Δ355–833) containing forward and inverted orientations of inserted LGH52/53 oligonucleotides encoding IE175 NLS 726-GRKRKSP-732 (pMM6a and pMM6b); (g and h) IE175(Δ355–833) containing forward and inverted orientations of inserted oligonucleotides LGH155/157 encoding IE110 500-VRPRKRR-506 (pMM8a and pMM8b). Protein products in panels a, b, d, and h were detected with 58S mouse anti-IE175(C) MAb; those in panels c, e, f, and g were detected with rabbit anti-IE175(N) PAb.

IE175(*tm*1029) truncation mutants all gave close to 85% exclusively nuclear expression, with approximately 5% of the cells showing predominantly cytoplasmic expression (i.e., 82%/5% N/C ratios). In contrast, the IE175(Δ355–833) deletion gave 80% fully cytoplasmic patterns, with no cells showing exclusively nuclear expression (0%/80% N/C ratio). Insertion of IE175 codons 726-GRKRKSP-732 gave a 63%/6% N/C ratio for one forward-oriented clone and a 97%/0% N/C ratio

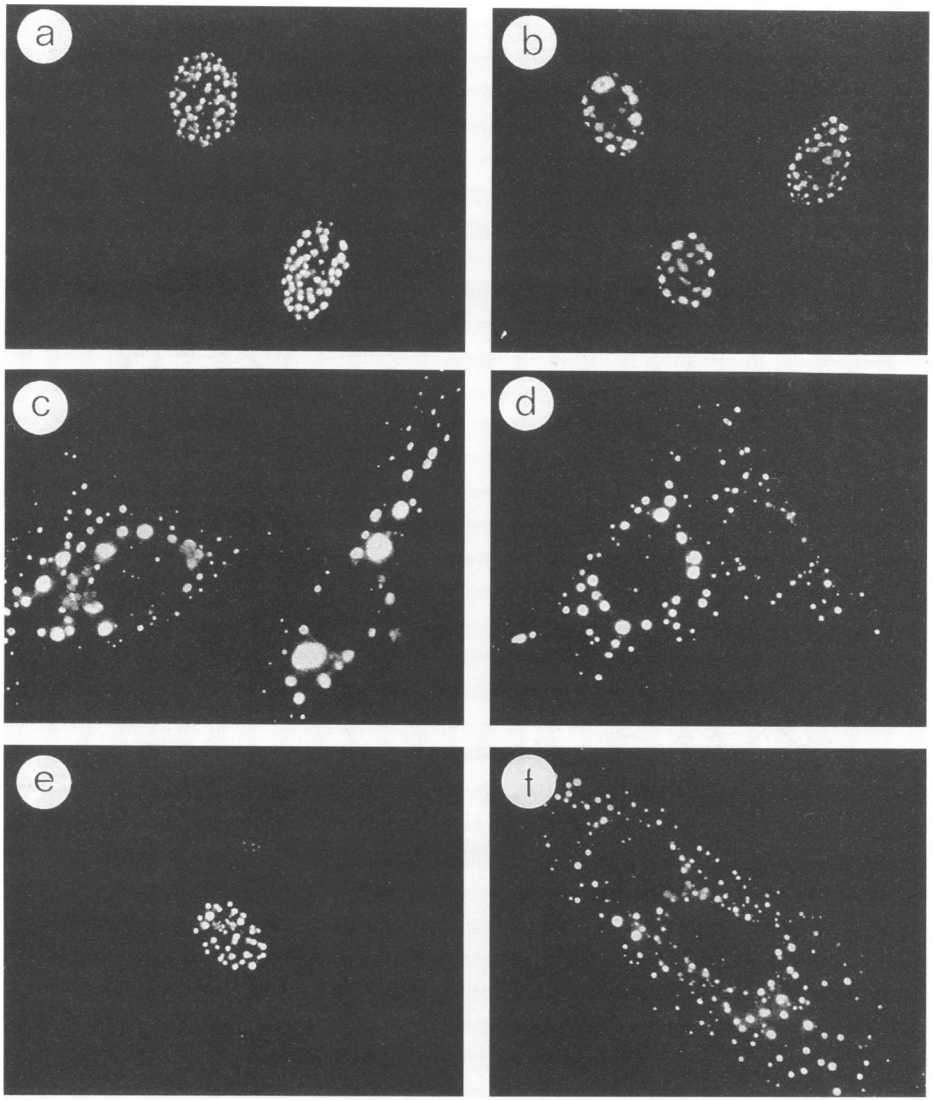

FIG. 2. Punctate distribution of IE110 and identification of an NLS. The photomicrographs show the results of IFA on DNA-transfected Vero cells receiving the following effector plasmids: (a) wild-type nuclear punctate IE110(1–775) encoded by plasmid pGH92; (b) wild-type nuclear IE110(1–775) expressed from an SCMV enhancer-driven effector plasmid pGH94; and (c and d) cytoplasmic punctate IE110(Δ365–517) from pMM63. (e) Restoration of nuclear characteristics to IE110(Δ365–517) after insertion of the LGH155/157 oligonucleotide pair encoding IE110 NLS 500-VRPRKRR-506 (pGH85a). (f) Inverted orientation of the same oligonucleotide into the IE110(Δ365–517) protein (pGH85b). The IE110 protein in panel a was detected with mouse H1053 MAb; those in panels b to f were detected with rabbit anti-IE110(N) PAb.

for another (Fig. 1e). An inversion of the inserted oligonucleotide failed to change the pattern from that of the deleted parent (0%/81% N/C ratio; Fig. 1f).

The putative IE110 NLS motif from codons 500-VRPRKRR-506 gave predominantly nuclear products with somewhat lower karyophilic properties than the IE175 motif in two forward-oriented inserts (Fig. 1g; N/C ratios of 52%/4% and 38%/5%), whereas two inverted inserts did not (Fig. 1h; N/C ratios of 0%/89% and 0%/87%). A second plausible potential IE175 NLS motif from codons 164-PPRRRRA-170 was negative (Fig. 1d), giving N/C ratios of 0%/82%, 0%/82%, and 0%/79% with three forward-oriented clones, and a putative signal from codons 152-PARRTRKP-159 of the EBV Zta transactivator was also negative, giving N/C values of 0%/87% and 0%/70% for two forward-oriented clones (Table 1, experiment 2).

Finally, the IE110 codon 500-to-506 NLS motif was inserted back in frame into the IE110(Δ364–518) background (Table 2, experiment 2) and found to restore nuclear localization to the same degree (42%/0% N/C ratio) as in the deleted IE175 background when in the forward orientation (Fig. 2e) but to have no effect in the backward orientation (Fig. 2f). Therefore, although we have not made specific point mutations to prove that these are the only NLS motifs in these two proteins, the signals that we have identified, namely, 726-GRKRKSP-732 in IE175 and 500-VRPRKKR-506 in IE110, are clearly both necessary and sufficient for correct nuclear localization within their natural contexts.

Mapping of the IE110 punctate characteristics. The typical smooth spherical punctate pattern of the intact IE110 nuclear distribution (Fig. 2a and b) was subtly altered in many of the deletion mutants. IE110(Δ365–517) displayed a relatively nor-

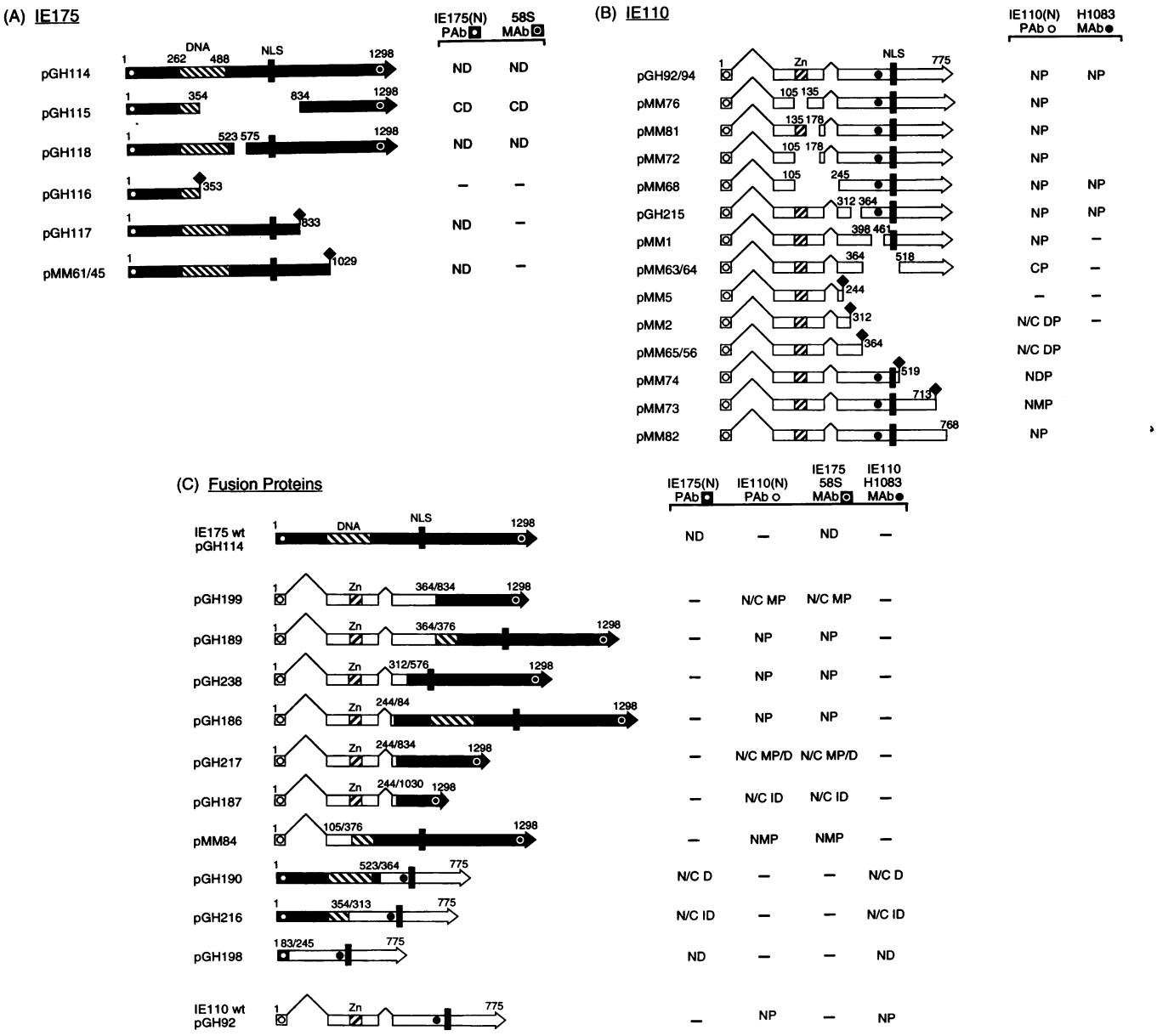

FIG. 3. Structures of IE175 and IE110 deletion mutants and hybrid proteins and summary of their intracellular distribution patterns. The diagrams illustrate the relative positions and codon numbers of internal deletions and truncation sites within the HSV-1 transactivator protein coding regions of the effector plasmids shown. (A) IE175 variants; (B) IE110 variants; (C) panel of in-frame IE110/IE175 and IE175/IE110 hybrid proteins. Solid and open horizontal bars denote IE175 and IE110 coding regions, respectively. Short vertical solid lines indicate defined NLS motifs, and hatched bars represent the zinc finger region in IE110 and the DNA-binding domain in IE175. Open and solid circles denote the approximate locations of defined PAb and MAb epitopes, respectively. ◆, inserted triple terminator oligonucleotide. The corresponding columns on the right summarize the results of IFA analysis in transient DNA transfection assays using the indicated antibodies. N, nuclear; C, cytoplasmic; N/C, mixed nuclear and cytoplasmic; D, diffuse; P, punctate; MP, micropunctate; ID, diffuse with irregular aggregates; –, negative results (absence of epitope or lack of expression).

mal punctate pattern, except that the granules were larger and localized almost exclusively in the cytoplasm (Fig. 2c and d). Furthermore, insertion of the 500-VRPRKRR-506 NLS motif back into this construction gave a nuclear punctate pattern similar to that of the wild-type gene (Fig. 2e). The internal deletions in exon 2 of IE110(Δ106–134), IE110(Δ136–177), and IE110(Δ106–177) showed somewhat novel IFA and phase-dense patterns with more irregular granules than usual, but they were still all basically nuclear punctate (Fig. 5a and b), with occasional cells showing stringy cytoplasmic patterns as well. IE110(Δ106–244) also remained punctate but sometimes gave a distinct pattern of elongated granules in the nucleus (10).

IE110(Δ313–363) and IE110(Δ399–460) both showed very typical nuclear punctate patterns (Fig. 5c). However, among the C-terminal truncation mutants, only IE110(*fs*768) was unaffected (not shown). The pattern with IE110(*tm*519) was predominantly diffuse, but with a small number of scattered

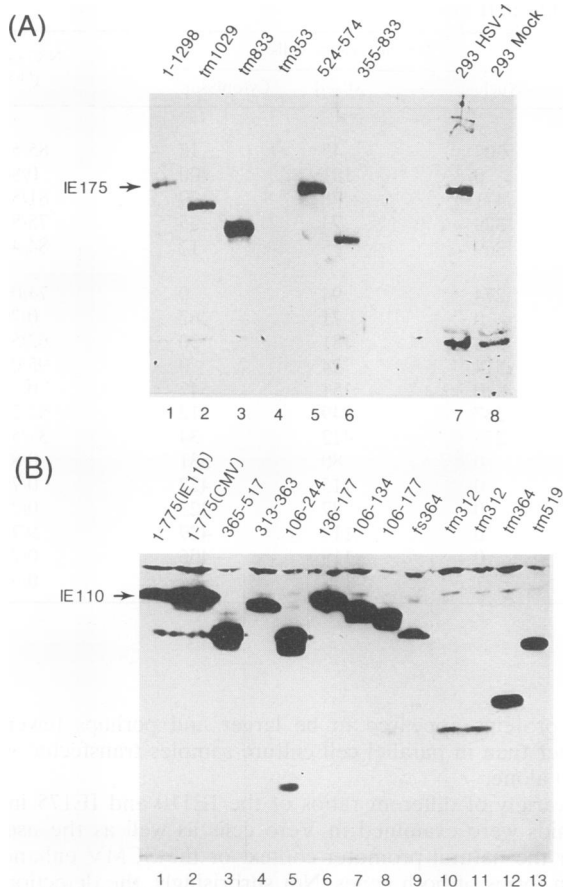

FIG. 4. Western immunoblotting to assess the sizes and abundance of IE175 and IE110 deletion and truncation variants produced in short-term expression assays. Whole-cell lysates of unlabeled protein were prepared from DNA-transfected 293 cells. After fractionation on SDS–7.5% polyacrylamide gels, the proteins were transferred to nitrocellulose and incubated with rabbit PAb plus alkaline phosphatase (A)- or HRP (B)-conjugated anti-IgG antibody. (A) Detection of IE175-related polypeptides with anti-IE175(N) PAb. Lanes: 1, IE175(1–1298) from pGH114; 2, IE175(*tm*1030) from pMM61; 3, IE175(*tm*833) from pGH117; 4, IE175(*tm*353) from pGH116; 5, IE175(Δ524–574) from pGH118; 6, IE175(Δ355–833) from pGH115. Controls consisted of samples from HSV-1(MP) infected 293 cells (lane 7) and mock-infected 293 cells (lane 8). (B) Detection of IE110-related polypeptides with anti-IE110(N) antipeptide PAb. Expected polypeptide sizes based on DNA sequence predictions of open reading frames are given in parentheses. Lanes: 1, IE110(1–775) from pGH92 (IE110 promoter) (86 kDa); 2, IE110(1–775) from pGH94 (SCMV promoter) (86 kDa); 3, IE110(Δ365–517) from pMM63 (69 kDa); 4, IE110(Δ313–363) from pGH215 (79 kDa); 5, IE110(Δ106–244) from pMM68 (70 kDa); 6, IE110(Δ136–177) from pMM81 (84 kDa); 7, IE110(Δ106–134) from pMM76 (80 kDa); 8, IE110(Δ106–177) from pMM72 (78 kDa); 9, IE110(*fs*364) from pMM56; 10, IE110(*tm*312) from pMM2 (34 kDa); 11, IE110(*tm*312) from pMM3 (34 kDa); 12, IE110(*tm*364) from pMM65 (40 kDa); 13, IE110(*tm*519) from pMM74 (57 kDa).

punctate spots in most cells (not shown). Both IE110(*tm*364) and IE110(*fs*364), together with the few positive cells obtained with IE110(*tm*312), also gave mixtures of phase-dense punctate or micropunctate and diffuse patterns as well as being mixed nuclear and cytoplasmic (Fig. 5e to g). In contrast, IE110(*tm*713) produced a nuclear micropunctate pattern with numerous small spherical granules overlaying a diffuse background (Fig. 5h). The micropunctate structures were still all detectable as tiny dense granules by phase microscopy. These results, which are summarized in Fig. 3B, imply that the signal for the punctate characteristics resides either between codons 1 and 105 or between codons 245 and 312. Additional minor influences contributing to the shape and number of the granules must also be provided by the zinc finger domain in exon 2 and from the codon 518 to 712 region in exon 3.

Transfer of the punctate characteristic to IE175 hybrid proteins. The observations described above were somewhat contradictory and surprising, given several previous analyses of these effects by other groups, which had implied that the extreme C terminus was the most critical portion of IE110 for the punctate characteristics (9, 17). For this reason, together with the fact that our conclusion about the role of an N-terminal domain being critical was based more on negative rather than on positive effects, we carried this analysis a step further. The experimental design essentially examined whether N-terminal or C-terminal segments of IE110 could transfer the punctate feature onto a hybrid protein containing IE175 sequences. Two principal series of hybrid genes were constructed (Fig. 3C). In the first set, N-terminal portions of IE110 were fused in frame in front of C-terminal portions of IE175; in the second set, C-terminal portions of IE110 were fused in frame downstream of N-terminal portions of IE175. In most cases, the fusions were generated by insertion of *Bgl*II linkers in each reading frame at the same restriction sites used to produce triple terminator truncations in each protein, followed by selection of appropriate matching reading frame versions for creating the hybrids. The availability of antibodies to both the N- and C-terminal regions of each protein provided great flexibility for analysis of the protein products by standard indirect IFA in DNA-transfected cells.

A series of seven IE175-based hybrid proteins with N-terminal regions from IE110 exchanged for those of IE175 was created (Fig. 3C). All were detectable with both anti-IE110(N) PAb and 58S anti-IE175 MAb. The four that included the NLS from codons 726 to 732 in IE175 were exclusively nuclear, although surprisingly, the other three hybrid proteins in this series, which lacked the standard NLS motifs from either gene but included the IE110 zinc finger domain, gave a mixed nuclear and cytoplasmic pattern (Table 2, experiment 3). Importantly, most of these constructions displayed an unambiguously punctate pattern in many or all positive cells (Fig. 6a, b, c, g, and h), although occasionally aberrant large globular or stringy patterns were also observed. IE110(1–244)/IE175 (1030–1298), which contained the shortest C-terminal segment from IE175, represented the only exception producing a diffuse pattern (Fig. 6d) that was often irregular or stringy. The most dramatically IE110-like punctate pattern was obtained when the 58S IE175 MAb was used to detect the IE110(1–244)/IE175(84–1298) hybrid protein, which encodes almost the full length of IE175 (pGH186; Fig. 6b and g), and with the IE110(1–312)/IE175(576–1298) hybrid protein (pGH238; Fig. 6a). Furthermore, these versions displayed the typical IE110 characteristic of phase-dense globular particles as well (not shown). Some of the other hybrid proteins containing N-terminal segments of IE110 gave significantly fewer or smaller punctate granules than the typical size observed with the intact wild-type IE110 gene in parallel experiments, and the pattern resembled the micropunctate pattern seen with IE110(*tm*364) and IE110(*tm*713) (Fig. 5h). All of these hybrids frequently gave a diffuse background also in Vero cells, which was similar to the effect seen with the IE110 truncation mutants. However, in 293 cells, the results were virtually indistinguishable from that of the wild-type IE110 pattern, with smooth-surfaced

TABLE 1. Identification of NLSs in IE175

Expt	Plasmid	Gene or insert	No. of positive cells[a]			N/C ratio (%)
			Nuclear	Mixed	Cytoplasmic	
1	Deletions and truncations					
	pGH114	IE175(1–1298)	303	43	18	85/5
	pGH115	IE175(Δ355–833)	0	101	400	0/80
	pMM45	IE175(*tm*1030)	471	78	29	81/5
	pGH117	IE175(*tm*833)	324	73	35	75/8
	pGH118	IE175(Δ524–574)	369	55	17	84/4
2	Oligonucleotide insertions					
	pGH114	IE175(1–1298)	274	94	0	74/0
	pGH115	IE175(Δ355–833)	0	71	262	0/79
	pMM6a1	GRKRKSP (IE175)[b]	344	181	30	62/5
	pMM6a2	GRKRKSP (IE175)[b]	514	24	0	95/0
	pMM6b1	GLLRLR (reverse)[b]	0	151	547	0/78
	pMM8a1	VRPRKRR (IE110)[b]	287	249	12	52/2
	pMM8a3	VRPRKRR (IE110)[b]	273	412	34	37/5
	pMM8b2	WRLFLGR (reverse)[b]	0	80	531	0/87
	pMM20a1	PPRRRRH (IE175)[b]	0	115	427	0/79
	pMM20a2	PPRRRRH (IE175)[b]	0	87	323	0/79
	pMM20a3	PPRRRRH (IE175)[b]	0	118	429	0/78
	pMM14a1	PARRTRKP (Zta)[b]	0	119	406	0/77
	pMM14a2	PARRTRKP (Zta)[b]	1	117	267	0/69

[a] All experiments were carried out in Vero cells.
[b] Added at deletion site in pGH115.

spherical punctate granules and little or no diffuse background (Fig. 6g and h). The IE110(1–105)/IE175(376–1298) hybrid protein (encoded by pMM84) was particularly intriguing because it displayed a mostly uniform diffuse pattern with some punctate granules in Vero cells (Fig. 6e) but in contrast gave a pattern consisting exclusively of smooth spherical micropunctate granules in 293 cells (Fig. 6h).

Three reciprocal IE110-based hybrids containing the N terminus of IE175 exchanged for the N terminus of IE110 (Fig. 3C) were also tested by using both the IE175(N) PAb and either the H1083 MAb or an IE110(C) PAb described by Ciufo et al. (10). In both Vero and 293 cells, these proved to give either exclusively diffuse nuclear products for IE175(1–83)/IE110(245–775) (Fig. 6f) or diffuse nuclear-plus-cytoplasmic products for IE175(1–354)/IE110(313–775) and IE175(1–523)/IE110(364–775). With all three of these constructions, there was also a tendency to much lower expression efficiency than usual and, for IE175(1–354)/IE110(313–775) in particular, the formation of large aggregates (10). However, importantly, all three products that contained the intact C-terminal half of IE110 failed to demonstrate any significant punctate characteristics (summarized in Fig. 3C). Therefore, we conclude that the ability to transfer the full IE110-like punctate feature to the IE175 protein clearly resides within the N-terminal portion of IE110. Codons 1 to 244 encompass the complete phenotype, and codons 1 to 105 produce a partial phenotype.

Redistribution of IE175 in IE110-cotransfected cells. Unexpectedly, transfection of both the wild-type IE175 and IE110 expression plasmids together into the same Vero cell cultures revealed that the normally exclusively diffuse IE175 pattern detected with 58S MAb became a mixture of the diffuse and punctate nuclear distribution types (Fig. 7f). This effect occurred in 30 to 50% of the positive cells and was not caused by cross-reaction of the IE175 antibody with IE110 or vice versa (Fig. 7a to d). Furthermore, the punctate IFA pattern detected with the IE175 antibody in these mixtures corresponded precisely to the number and location of phase-dense granules seen in the same cells (Fig. 8e and f; Fig. 9a and b). In general, the nuclear punctate granules in cotransfected cells expressing both proteins appeared to be larger and perhaps fewer in number than in parallel cell culture samples transfected with IE110 alone.

A variety of different ratios of the IE110 and IE175 input plasmids were examined in Vero cells as well as the use of either the natural promoter context or the SCMV enhancer-driven forms of both genes. Not surprisingly, the detection of proteins recognized by the IE175 antibody in punctate granules was greatest at the highest ratios of IE110 to IE175 and in the combination of the SCMV-driven IE110 gene (pGH94) together with the IE175 natural promoter context IE175 (p*Xho*I-C). At the highest ratios, many cells expressed only IE110, as judged by the presence of phase-dense granules in cells that failed to display any immunofluorescence with the anti-IE175 antiserum (Fig. 8c and d), but almost all (90%) of the cells that were positive for IE175 showed both punctate and diffuse patterns (Fig. 8e and f). At the opposite extreme, the localization of the product detected with the IE110-specific antibody was only rarely altered in a reciprocal fashion from the standard nuclear punctate distribution to a diffuse IE175-like pattern, even when most of the positive cells also expressed IE175. Evidently, the IE110 punctate phenotype dominates over that of IE175, presumably because the former involves a specific signaling motif that is active even when in a complex or aggregate with IE175 proteins lacking the signal.

Lack of interaction between IE110 and the cotransfected IE72 nuclear protein of HCMV. To judge whether the ability of IE110 to drag the IE175 protein into punctate structures was a specific effect rather than possible nonspecific trapping, we repeated the experiment by using a plasmid (pRL45) encoding the nuclear IE72 (IE1) and IE82 (IE2) protein products of HCMV, which display an intracellular distribution similar to that of IE175 with a uniform diffuse nuclear pattern including sparing of the nucleoli (31). Parallel control samples receiving IE175 cotransfected together with a deleted but still nuclear punctate form of IE110 (pGH215) revealed an unambiguous colocalization with phase-dense punctate granules in up to 50% of the IE175 positive nuclei (Fig. 9a and b). However, when cotransfected with wild-type nuclear IE110, the typical

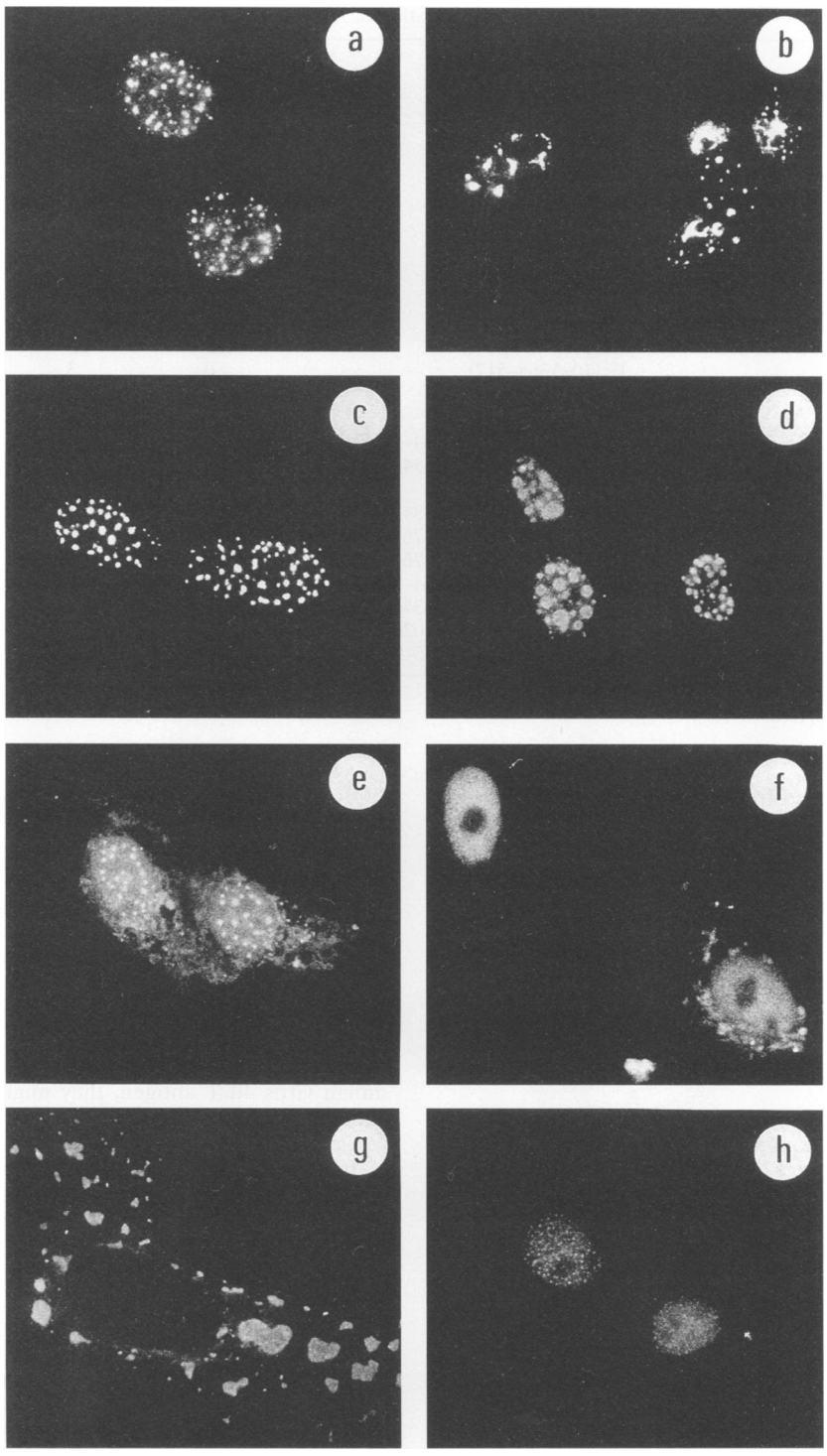

FIG. 5. Intracellular distribution of various deleted and truncated forms of IE110. The photomicrographs show representative DNA-transfected Vero cells after detection of IE110 protein products by IFA with anti-IE110(N) PAb. (a) IE110(Δ106–134) expressed from pMM76; (b) IE110(Δ136–177) from pMM81; (c) IE110(Δ313–363) from pGH215; (d) IE110(Δ399–460) from pMM1; (e and g) nuclear and cytoplasmic examples of IE110(*fs*364) from pMM56; (f) IE110(*tm*364) from pMM65; (h) IE110(*tm*713) from pMM73.

pattern of IE72 diffuse nuclear immunofluorescence was unaltered in any of 500 screened positive nuclei when detected with the appropriate HCMV-specific MAb (Fig. 9c). Confirmation of the expression of IE110 in many of the same cells that were positive for IE72 was accomplished by detection of IE110-like phase-dense granules (Fig. 9d). In fact, a comparison of the IE72-specific MAb distribution with that of phase-dense granules in the same cotransfected cells gave the distinct impres-

TABLE 2. Identification of NLSs in IE110

Expt	Plasmid	Gene or insert	No. of positive cells[a]			N/C ratio (%)
			Nuclear	Mixed	Cytoplasmic	
1	Deletions and truncations					
	pGH92	IE110(1–775)	528	148	0	72/0
	pGH94	SCMV IE175(1–775)	207	118	0	65/0
	pMM74	IE110(*tm*364)	9	105	2	8/2
	pMM68	IE110(Δ106–244)	120	2	4	95/3
	pGH215	IE110(Δ313–363)	267	52	0	80/0
	pMM1	IE110(Δ399–460)	278	50	0	82/0
	pMM63	IE110(Δ365–517)	0	61	42	0/42
2	Oligonucleotide insertions					
	pGH92	IE110(1–775)	122	25	0	79/0
	pGH63	IE110(Δ365–517)	0	3	105	0/97
	pMM85a	VRPRKRR (IE110)[b]	66	93	0	42/0
	pMM85b	WRLFLGR (reverse)[b]	0	5	100	0/95
	pMM186	IE110(1–244)/IE175(84–1298)	62	0	0	100/0
	pMM84	IE110(1–105)/IE175(354–1298)	64	7	0	90/0
3	Hybrid proteins					
	pGH199	IE110(1–364)/IE175(834–1298)	101	181	2	35/1
	pGH189	IE110(1–364)/IE175(376–1298)	503	180	7	73/1
	pGH238	IE110(1–312)/IE175(576–1298)	81	3	0	96/0
	pGH186	IE110(1–244)/IE175(84–1298)	611	62	0	89/0
	pGH217	IE110(1–244)/IE175(834–1298)	127	132	13	46/5
	pGH187	IE110(1–244)/IE175(1020–1298)	639	100	1	86/0
	pGH198	IE175(1–83)/IE110(245–775)	148	6	0	96/0

[a] All experiments were carried out in Vero cells.
[b] Added at deletion site in IE110(Δ365–517).

sion that IE72 was excluded from these locations. Additional cotransfection experiments were carried out with a plasmid encoding the HCMV IE72 protein only (pMP17) at several different ratios of IE110 to IE72 without any effect on the IE72 uniform diffuse IFA patterns. Similar control cotransfection experiments have failed to detect any interaction between IE110 and the nuclear ICP8 (SSB or UL29) protein of HSV (data not shown). Therefore, the IE110-IE175 interaction is not a simple nonspecific trapping phenomenon.

DISCUSSION

NLSs in herpesvirus IE proteins. Our results have clearly defined the single most dominant nuclear localization signal motifs in both the IE175 and IE110 proteins of HSV-1. These motifs conform to the simple compact simian virus 40 T-antigen pattern (PKKKRKV), with four or five clustered basic amino acids, together with a Pro and nearby Ser or Thr amino acids (28). The IE110 NLS of 501-RPRKRRGS-508 is totally conserved at 510-RPRKRRGS-517 in the HSV-2 version but is not present in the same form in the very different equivalent proteins of varicella-zoster virus and pseudorabies virus. The IE175 NLS of 726-GRKRKSP-732 is also not directly conserved in the homologous varicella-zoster virus, equine abortion virus, or pseudorabies virus version of this protein, although several alternative potential functionally equivalent motifs are present. Primary amino acid data for HSV-2 IE175 are not yet available. We have previously reported positive results in the same IE175(Δ355–833) karyophilic motif test system for both 145-PRKKPRK-151 (NLS-1) and 321-PRKKKSKR-328 (NLS-2) of HCMV IE2 (45) and for the single predominant NLS motifs at 379-KRPRSPSS-387 in EBNA-1 (2) and at 478-SKRPRPS-485 in EBNA-2 (33) from EBV. Negative results were obtained with EBNA-1 71-RRPQKRP-77 and 394-SPPRRPPPGRRP-405, and very weak positive results were obtained with EBNA-2 356-GKGKSRD KQRKPG-368. The present negative result with the IE175 164-PPRRRRA-170 motif is probably best explained by the apparent rule that at least one basic amino acid must be a Lys. Our negative result with the Zta 152-PARRTRKP-159 motif was more of a surprise but can now be explained following a recent analysis suggesting that this latter sequence alone represents just one section of a bipartite NLS in Zta (36). Note that both the identified IE175 and IE110 NLS motifs and several of the others would be expected to be targets for protein kinase A and possibly also protein kinase C, which raises the interesting possibility that, like the classical motif in simian virus 40 T antigen, they might be regulated by phosphorylation events (47).

An earlier report by Everett (17) had narrowed the location of the IE110 NLS motif to between codons 475 and 549. Similarly, the best mapping data reported for the location of IE175 NLS placed it between amino acids 682 and 774 (12, 13, 42). However, no direct evidence for the precise identification of either of these motifs has been presented previously. Our studies also appear to eliminate the possibility of additional independent motifs beyond the 354-to-834 boundaries for IE175 and beyond the 364-to-398 or 461-to-518 boundaries in IE110. However, in IE175 in particular, we cannot exclude the possibility that the untested adjacent sequence 743-PRPPKT KKS-751 mapping just to the right of our positive motif has independent NLS properties also.

In Everett's studies (17), IE110 proteins with deletions spanning amino acids 424 to 549, 475 to 549, 348 to 509, and 509 to 638 were all cytoplasmic, but those spanning 389 to 474 and 541 to 548 were nuclear. Consequently, he concluded that the basic motif alone could not be sufficient to convey this characteristic. Although insertion of IE110 amino acids 500-VRPRKRR-506 alone restored nuclear localization to both of our test proteins, i.e., IE175(Δ355–833) and IE110(Δ365–517), its karyophilic properties were not as efficient as those of the IE175 NLS motif. Conceivably, the absence of the conserved

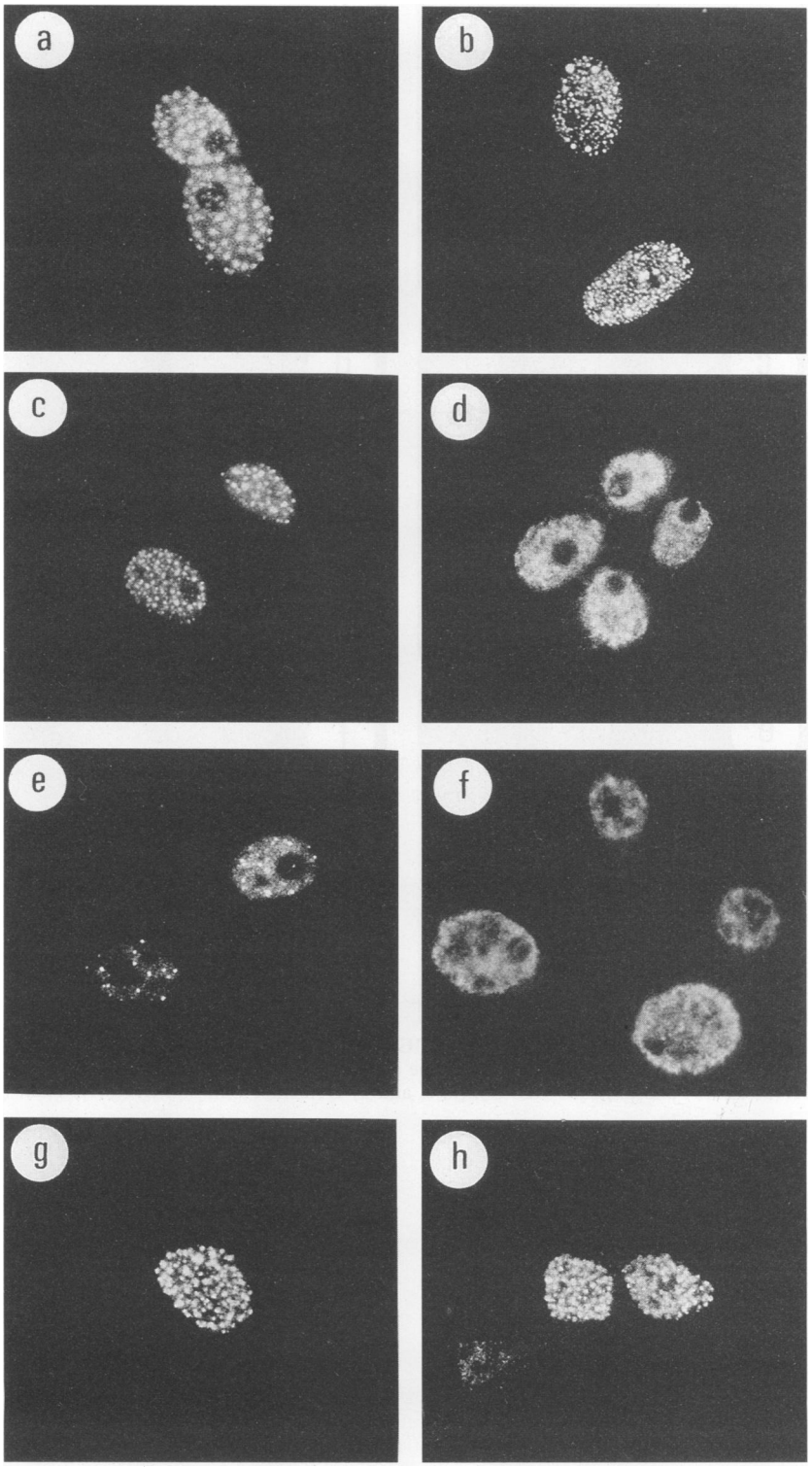

FIG. 6. Transfer of punctate characteristics to IE110/IE175 hybrid proteins. IFA was carried out after transient DNA transfection into either Vero cells (a to f) or 293 cells (g and h). (a) IE110(1–312)/IE175(576–1298) hybrid protein expressed from pGH238; (b) IE110(1–244)/IE175(84–1298) encoded by pGH186; (c) IE110(1–364)/IE175(376–1298) from pGH189; (d) IE110(1–244)/IE175(1030–1298) from pGH187; (e) IE110(1–105)/IE175(354–1298) from pMM84; (f) IE175(1–83)/IE110(245–775) from pGH198; (g) IE110(1–244)/IE175(84–1298) from pGH186; (h) IE110(1–105)/IE175(354–1298) from pMM84.

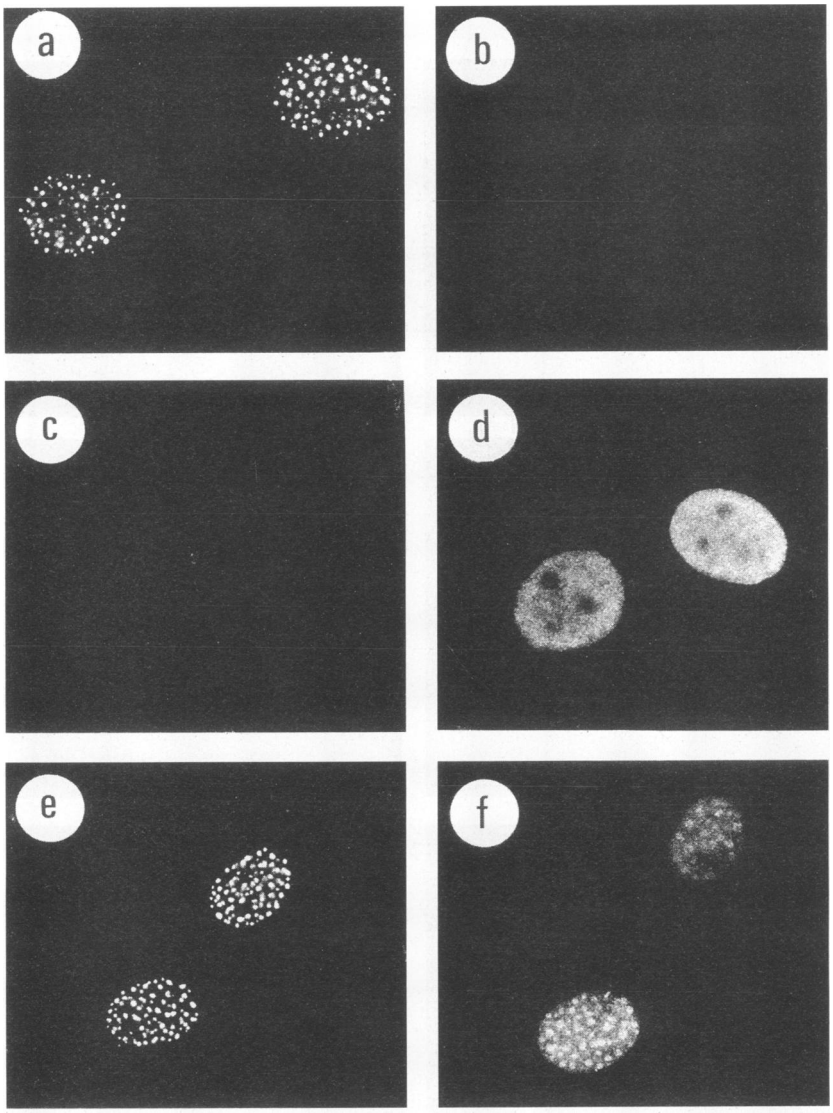

FIG. 7. Altered IE175 distribution pattern after cotransfection with IE110. The photomicrographs show the results of IFA carried out in either singly transfected or cotransfected Vero cells. (a and c) IE110 wild type encoded by pGH92; (b and d) IE175 wild type encoded by p*Xho*I-C; (e and f) cotransfection of pGH92 (IE110) and p*Xho*I-C (IE175). (a, c, and e) Detection with anti-IE110(N) PAb; (b, d, and f) detection with anti-IE175(N) PAb.

adjacent Gly and Ser amino acids at 507 and 508, which could provide a protein kinase target site, may have contributed to this effect. However, in our studies, the deletion from 365 to 517 was fully cytoplasmic and the termination mutant at 519 was fully nuclear. Therefore, the only additional adjacent amino acids that could contribute must lie between codons 509 and 518. Perhaps the best explanation may be either that deletion beyond 509 disrupts a larger nonessential extension of the basic motif or, more likely, that Everett's 509-to-638 deletion (17) may happen to juxtapose the basic motif into a nonfunctional context. Note that removal of the IE110 NLS motif at codons 500 to 506 by truncation at position 312 or 364 still resulted in a mixed nuclear-cytoplasmic product, and indeed, some of our hybrid IE110/IE175 proteins that did not contain any of the identified NLS motifs from either parent protein nevertheless displayed a predominantly nuclear or mixed nuclear-plus-cytoplasmic distribution (Fig. 3C and 5). Evaluation of these constructions suggests that the IE110 exon 2 region encompassing the zinc finger domain may also have some limited nuclear localization targeting characteristics, especially in the absence of the C-terminal segment of the protein.

Mapping of the domain responsible for the IE110 punctate characteristics. Our interpretations differ from those of both the Everett and Silverstein groups, who concluded from previous results with truncation and insertion mutants that the C terminus of IE110 is of greatest importance for encoding the IE110 punctate characteristics (9, 17). We agree that the C terminus contributes to the punctate effect, especially with IE110(*tm*519), which is the least punctate of our deletion mutants. However, the positive effects of transferring the full phenotype to an IE175 hybrid protein provides a compelling argument that a domain specifying the punctate feature resides within the N terminus.

In Everett's studies, IE110 proteins with deletions at positions 633 to 680, 680 to 720, 696 to 723, and 723 to 767 were all

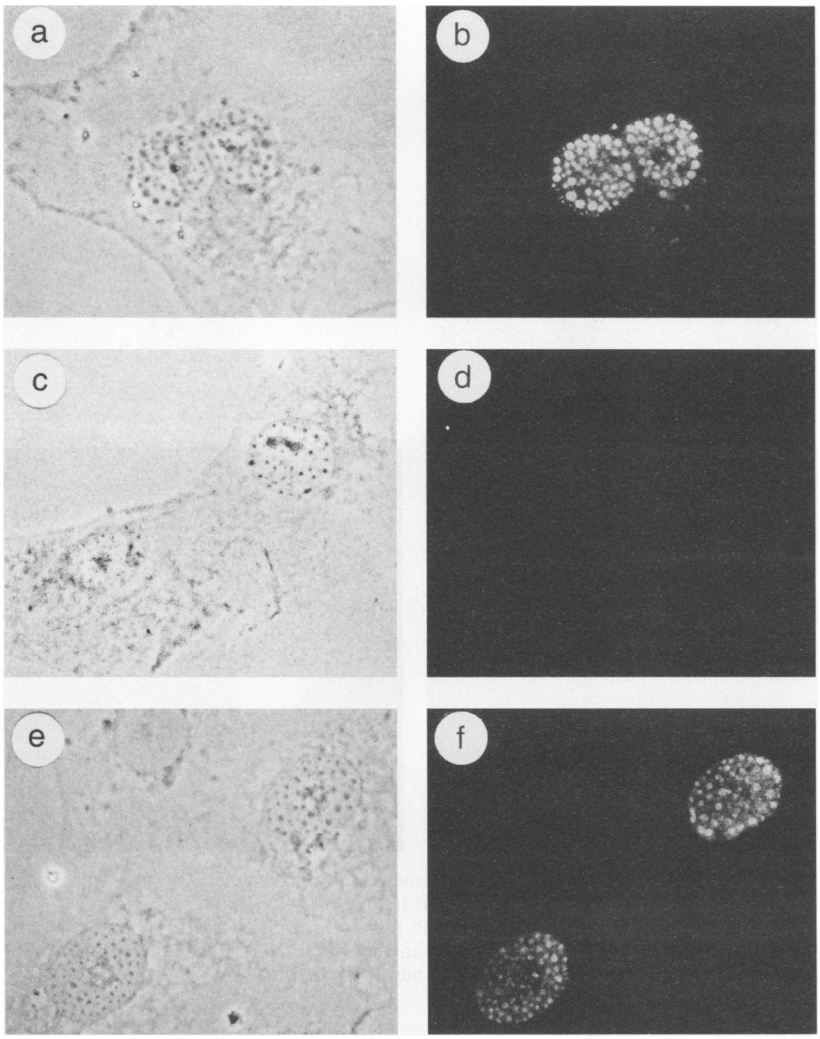

FIG. 8. Colocalization of HSV IE175 with punctate granules in IE110-cotransfected cells. (a and b) Control colocalization of wild-type nuclear IE110 protein with phase-dense granules in pGH92-transfected Vero cells. The figure shows a comparison of the same field of two nuclei, using phase-contrast photomicroscopy (a) and IFA photomicroscopy after detection with FITC-conjugated anti-IE110(N) PAb (b). (c and d) Absence of IFA signal associated with IE110 punctate granules expressed in pGH92-transfected cells when incubated with control anti-IE175 antibody. The photomicrographs show the same two cells under phase contrast (c) and after IFA with FITC-conjugated anti-IE175(N) PAb (d). (e and f) Colocalization of IE175 with IE110 punctate granules in cells that received both the p*Xho*I-C and pGH92 plasmids. The photomicrographs show the same two cotransfected nuclei under phase contrast (e) and after IFA with anti-IE175(N) PAb (f).

reported to give either diffuse nuclear patterns or tiny spots (17). Similarly, in the study of Chen et al. (9), IE110 proteins with deletions covering positions 628 to 697 and 628 to 769 appeared to give diffuse patterns. We obtained generally similar results with truncation mutant IE110(*tm*712), which gave a distinct micropunctate pattern, and with IE110(*tm*519), which produced a predominantly diffuse pattern with only occasional punctate globules. However, both IE110(*tm*312) and IE110(*tm*364) gave mixed nuclear and cytoplasmic and mixed micropunctate and diffuse patterns. Initially, two possible alternative explanations seemed plausible, either (i) the primary determinant of the punctate characteristic lies toward the N terminus or (ii) the triple terminators at 312 and 364 were being partially bypassed by putative alternative splicing events that brought the C-terminal domain back in frame.

Because shorter N-terminal versions of IE110 (and also IE175) were unstable, we reasoned that the best approach at this point would be to examine directly whether the N- or C-terminal portion of IE110 could transfer the punctate phenotype to an IE175 protein. The results of IFA with a range of these hybrid constructions revealed that exchange of the IE110 N-terminal segments alone could convert IE175 to a protein with a totally punctate distribution pattern, whereas the reciprocal exchange of C-terminal segments failed to do so. For example, the hybrid protein with IE110(1–244) added in frame in front of IE175(84–1298) behaved almost exactly like wild-type IE110 by giving crisp exclusively punctate nuclear IFA with the 58S anti-IE175 MAb and producing directly visible phase-dense granules in transfected cells. In contrast, the exactly reciprocal hybrid protein consisting of IE175(1–83)/IE110(245–775) gave the standard IE175 diffuse nuclear pattern when detected with the anti-IE110 MAb.

The simplest and most satisfactory explanation must be that indeed the N terminus of IE110 specifies the property of punctateness, but that the C terminus provides some feature that contributes to the full punctate phenotype in an IE110

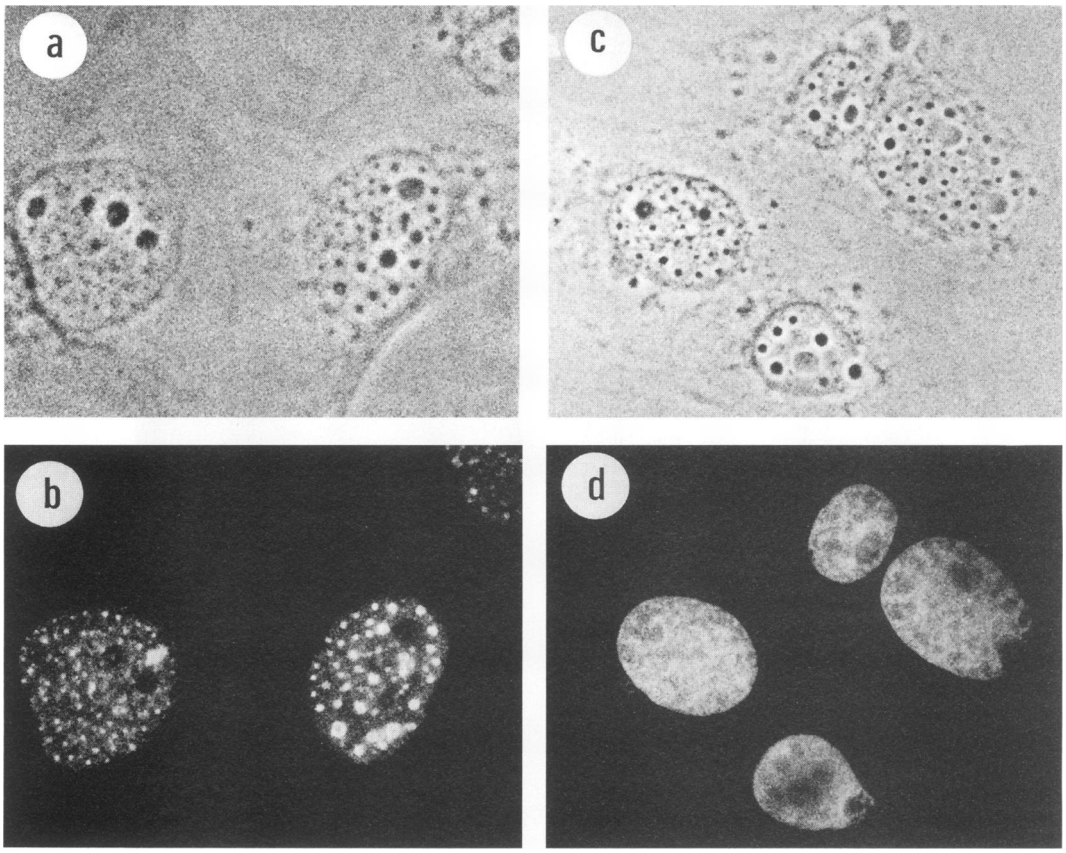

FIG. 9. Lack of association of HCMV IE72 with IE110 punctate granules in cotransfected cells. (a) Control phase-contrast photomicrograph showing IE110 punctate granules in Vero cells cotransfected with nuclear IE110(Δ313–363) from pGH215 and wild-type IE175 from p*Xho*I-C; (b) IFA detection of IE175 with IE175(N) PAb in the same field shown in panel a; (c) phase-contrast photomicrograph showing IE110 punctate granules in Vero cells cotransfected with nuclear IE110 from pGH92 and wild-type HCMV IE72 from plasmid pRL45; (d) IFA detection of HCMV IE72 with Chemicon mouse anti-MIE MAb in the same field shown in panel c.

context. Thus, IE175 must potentially also have some property that substitutes for that normally provided by the C terminus of IE110. A plausible explanation for the apparent loss of punctate character with some C-terminal IE110 truncation mutants is related to dimerization. We have shown elsewhere (10) that an IE110 homodimerization domain, which can be demonstrated by both in vitro coimmunoprecipitation and intracellular colocalization IFA, maps to between codons 617 and 711. Therefore, many of our IE110 deletions and truncations, except IE110(*tm*312), IE110(*tm*364), and IE110(*tm*519), should still be able to dimerize and the IE110(1–244)/IE175(84–1298) hybrid should also be in a dimeric form because it retains the intact DNA-binding and presumed dimerization domain from region B of IE175 (encompassing codons 262 to 488). Several of the other IE110/IE175 hybrid proteins that do not have a complete IE175 B region behave aberrantly with regard to either intracellular localization and stability or punctate characteristics, which probably correlates with either their inability to dimerize properly or some masking effects of C-terminal portions of IE175.

One obvious additional consequence of our model is that deletions in the N terminus of IE110 in front of the zinc finger domain should also lose the punctate characteristics. We have not tested this directly; however, one of the IE110 deletion proteins used by Everett (17) lacked amino acids 9 to 76 and apparently could not be detected or recognized by IFA, despite still being functional in transactivation studies (17). Similarly, two IE110 proteins used by Chen et al. (9), which lacked amino acids 11 to 106 or 106 to 212, both appeared to give aberrant diffuse IFA patterns. From our results, IE110 codons 1 to 244 are clearly sufficient to transfer the full punctate characteristic, including the phase-dense properties of the granules in both Vero and 293 cells, and codons 1 to 105 encompass a domain with at least a partial punctate phenotype. Curiously, the only well-conserved motifs between HSV-1 and HSV-2 within this latter region are two short acidic amino acid blocks that include the characteristic features of potential casein kinase II target sites (i.e., codons 35-DSSDSEAETEVG-46 and 55-DDDSASEADSTDTELFE-71 in HSV-1).

We do not yet know the significance of the punctate appearance of the isolated IE110 gene product. Undoubtedly, the largest granules shown in our photographs are to some degree an artifact of overexpression in DNA-transfected cells. However, it is worth pointing out that (i) these experiments were carried out under conditions identical to those that we used to demonstrate the functional properties of IE110 as a transcriptional transactivator (38, 39); (ii) the amount of IE110 produced in virus-infected cells is roughly equal to that synthesized in DNA-transfected cells, as judged by the intensity of the IFA signals, and (iii) in Vero cells transfected with the wild-type IE110 gene (pGH92), there are many cells that give only a weak (and hard to photograph) signal, but these still

display an IFA pattern that consists of scores of tiny micropunctate spots. Furthermore, at early stages of infection by wild-type HSV (i.e., 2 to 3 h after addition of virus), IE110 displays a similar nuclear and predominantly micropunctate IFA pattern, whereas IE175 gives a nuclear diffuse pattern (26a, 30). Both patterns become much more irregular and mixed beyond that stage, perhaps as a result of interactions with other proteins and eventually also because of incorporation of the IE175 protein (and possibly IE110 also) into virus DNA replication compartments (29). However, in infections at nonpermissive temperature with the HSV-1(17) IE175*ts*K mutant, in which nonfunctional nuclear IE175 remains uniform and diffuse but delayed-early products are not synthesized, the IE110 protein also remains localized in a predominantly punctate pattern in the nucleus (29). Occasionally, the punctate granules seen in DNA-transfected cells have the appearance of corresponding to nuclear pores, and they also resemble sites of c-*myc* localization, spliceosomes, and loci for initiation of DNA synthesis, which are all nuclear and punctate. However, the retention of the punctate spherical granule pattern in cytoplasmic forms of IE110 appears to rule out most of those options. Very likely the phase-dense characteristic implies that some highly abundant cellular proteins are also recruited into the sites where IE110 aggregates.

Possibility of IE110-IE175 interactions. We were able to exploit the distinctive punctate characteristics of the IE110 intracellular distribution pattern to demonstrate that the presence of IE110 in cotransfected cells leads to a dramatic redistribution of IE175 in many doubly expressing cells, with much of it now colocalized with the IE110 punctate granules. Knipe and Smith (30) observed that an HSV-1(STH2) virus carrying the IE175*ts*B2 mutation gave rise to a cytoplasmically located form of IE175 after infection at nonpermissive temperatures and that this appeared to prevent the wild-type IE110 protein from entering the nucleus. Potentially, those results can be explained by specific protein-protein interactions, although in subsequent transient assays, we have found that the nuclear IE110 protein has a considerably greater tendency to drag a cytoplasmic form of IE175 into the nucleus than vice versa (36a). The fact that cotransfection of the IE110 effector DNA together with plasmids encoding either the HCMV IE72 or HSV ICP8 nuclear protein failed to influence the uniform diffuse intranuclear distribution of those two proteins argues strongly against this phenomenon being caused by simple nonspecific stickiness of the IE110 protein. However, at present, we cannot rule out the possibility that the observed IE175-IE110 interaction is indirect, with some other cellular protein or proteins mediating the effect. In subsequent analyses, we have found that the ability of IE110 and IE175 to colocalize in cotransfected cells can be mapped to domains within the C-terminal segments of both proteins (36a). Furthermore, the HSV IE63 protein also proved to interact with IE110 in similar cotransfection IFA assays. Additional studies are in progress to attempt to confirm these properties in vitro and to evaluate the functional significance of these interactions.

ACKNOWLEDGMENTS

This research was funded by DHEW research grants R01 CA28473 and R37 CA22130 to G.S.H. from the National Cancer Institute. M.-A.M. was a visiting graduate student from the Department of Chemistry at the University of South Carolina.

We thank Mabel Chiu, Saswati Sinha, and Jane Gimigliano for excellent technical assistance with plasmid constructions, immunofluorescence experiments, and antiserum preparations at various stages of this work. We also thank Sarah Heaggans and Pamela Wright for help in photography and preparation of the manuscript.

REFERENCES

1. **Ackermann, M., D. K. Braun, L. Pereira, and B. Roizman.** 1984. Characterization of herpes simplex virus 1 α proteins 0, 4, and 27 with monoclonal antibodies. J. Virol. **52:**108–118.
2. **Ambinder, R. F., M. Mullen, Y.-N. Chang, G. S. Hayward, and S. D. Hayward.** 1991. Functional domains of Epstein-Barr virus nuclear antigen EBNA-1. J. Virol. **65:**1466–1478.
3. **Bachenheimer, S. L., and N. Elshiekh.** 1990. Variable requirements for herpes simplex virus immediate-early proteins in the expression of the adenovirus E2 gene. Virology **175:**338–342.
4. **Cai, W., and P. A. Schaffer.** 1989. Herpes simplex virus type 1 ICP0 plays a critical role in the de novo synthesis of infectious virus following transfection of viral DNA. J. Virol. **63:**4579–4589.
5. **Cai, W., and P. A. Schaffer.** 1991. A cellular function can enhance gene expression and plating efficiency of a mutant defective in the gene for ICP0, a transactivation protein of herpes simplex virus type 1. J. Virol. **65:**4078–4090.
6. **Cai, W., and P. A. Schaffer.** 1992. Herpes simplex virus type 1 ICP0 regulates expression of immediate-early, early, and late genes in productively infected cells. J. Virol. **66:**2904–2915.
7. **Chen, J., C. Panagiotidis, and S. Silverstein.** 1992. Multimerization of ICP0, a herpes simplex virus immediate-early protein. J. Virol. **66:**5598–5602.
8. **Chen, J., and S. Silverstein.** 1992. Herpes simplex viruses with mutations in the gene encoding ICP0 are defective in gene expression. J. Virol. **66:**2916–2927.
9. **Chen, J., X. Zhu, and S. Silverstein.** 1991. Mutational analysis of the sequence encoding ICP0 from herpes simplex virus type 1. Virology **180:**207–220.
10. **Ciufo, D. M., M.-A. Mullen, and G. S. Hayward.** 1994. Identification of a dimerization domain in the C-terminal segment of the IE110 transactivator protein from herpes simplex virus. J. Virol. **68:**3267–3282.
11. **Ciufo, D. M., C. apRhys, M. S. Roberts, and G. S. Hayward.** 1988. Viral and cellular factors involved in the regulation of the IE175 and IE110 promoters of herpes simplex virus, p. 95–111. Proceedings of the Symposium on Regulation of Viral Gene Expression. George Khoury Educational Foundation, Inc.
12. **DeLuca, N. A., A. M. McCarthy, and P. A. Schaffer.** 1985. Isolation and characterization of deletion mutants of herpes simplex virus type 1 in the gene encoding immediate-early regulatory protein ICP4. J. Virol. **56:**558–570.
13. **DeLuca, N. A., and P. A. Schaffer.** 1988. Physical and functional domains of the herpes simplex virus transcriptional regulatory protein ICP4. J. Virol. **62:**732–743.
14. **Everett, R. D.** 1984. Transactivation of transcription by herpes virus products: requirement for two HSV-1 immediate-early polypeptides for maximum activity. EMBO J. **3:**3135–3141.
15. **Everett, R. D.** 1987. A detailed mutational analysis of Vmw110, a trans-acting transcriptional activator encoded by herpes simplex virus type 1. EMBO J. **6:**2069–2076.
16. **Everett, R. D.** 1988. Promoter sequence and cell type can dramatically affect the efficiency of transcriptional activation induced by herpes simplex virus type 1 and its immediate-early gene products Vmw175 and Vmw110. J. Mol. Biol. **203:**739–751.
17. **Everett, R. D.** 1988. Analysis of the functional domains of herpes simplex virus type 1 immediate-early polypeptide Vmw110. J. Mol. Biol. **202:**87–96.
18. **Everett, R. D., A. Orr, and M. Elliot.** 1991. High level expression and purification of herpes simplex virus type 1 immediate-early polypeptide Vmw110. Nucleic Acids Res. **19:**6155–6161.
19. **Faber, S. W., and K. W. Wilcox.** 1988. Association of herpes simplex virus regulatory protein ICP4 with sequences spanning the ICP4 gene transcription site. Nucleic Acids Res. **16:**555–570.
20. **Fremont, P. S., I. M. Hanson, and J. Trowsdale.** 1991. A novel cysteine rich sequence motif. Cell **64:**483–484.
21. **Gelman, I. H., and S. Silverstein.** 1985. Identification of immediate early genes from herpes simplex virus that transactivate the virus thymidine kinase gene. Proc. Natl. Acad. Sci. USA **82:**5265–5269.
22. **Gelman, I. H., and S. Silverstein.** 1986. Co-ordinate regulation of herpes simplex virus gene expression is mediated by the functional interaction of two immediate early gene products. J. Mol. Biol. **191:**395–409.

23. **Gelman, I. H., and S. Silverstein.** 1987. Herpes simplex virus immediate-early promoters are responsive to virus and cell *trans*-acting factors. J. Virol. **61:**2286–2296.
24. **Harrigan-Mullen, M.-A.** 1991. Characterization of nuclear translocation, dimerization and IE110-IE175 interaction domains of the IE110 and IE175 proteins of HSV-1. Ph.D. thesis. The University of South Carolina, Columbia.
25. **Harris, R. A., R. D. Everett, X. Zhu, S. Silverstein, and C. M. Preston.** 1989. Herpes simplex virus type 1 immediate-early protein Vmw110 reactivates latent herpes simplex virus type 2 in an in vitro latency system. J. Virol. **63:**3513–3515.
26. **Hayward, G. S.** 1993. Immediate-early gene regulation in herpes simplex virus. Semin. Virol. **4:**15–23.

26a. **Hayward, G. S.** Unpublished data.

27. **Jeang, K.-T., D. R. Rawlins, P. J. Rosenfeld, J. H. Shero, T. J. Kelly, and G. S. Hayward.** 1987. Multiple tandemly repeated binding sites for cellular nuclear factor 1 that surround the major immediate-early promoters of simian and human cytomegalovirus. J. Virol. **61:**1559–1570.
28. **Kalderon, D., W. D. Richardson, S. F. Markham, and A. E. Smith.** 1984. Sequence requirements for nuclear location of simian virus 40 large-T antigen. Nature (London) **311:**33–38.
29. **Knipe, D. M., D. Senechek, S. A. Rice, and J. L. Smith.** 1987. Stages in the nuclear association of the herpes simplex virus transcriptional activator protein ICP4. J. Virol. **61:**276–284.
30. **Knipe, D. M., and J. L. Smith.** 1986. A mutant herpesvirus protein leads to a block in nuclear localization of other viral proteins. Mol. Cell. Biol. **6:**2371–2381.
31. **LaFemina, R. L., M. C. Pizzorno, J. D. Mosca, and G. S. Hayward.** 1989. Expression of the acidic nuclear immediate-early protein (IE1) of human cytomegalovirus in stable cell lines and its preferential association with metaphase chromosomes. Virology **172:**584–600.
32. **Leib, D. A., D. M. Coen, C. L. Bogard, K. A. Hicks, D. R. Yager, D. M. Knipe, K. L. Tyler, and P. A. Schaffer.** 1989. Immediate-early regulatory gene mutants define different stages in the establishment and reactivation of herpes simplex virus latency. J. Virol. **63:**759–768.
33. **Ling, P. D., J. J. Ryon, and S. D. Hayward.** 1993. EBNA-2 of herpesvirus papio diverges significantly from the type A and type B EBNA-2 proteins of Epstein-Barr virus but retains an efficient transactivation domain with a conserved hydrophobic motif. J. Virol. **67:**2990–3003.
34. **Metzler, D. W., and K. W. Wilcox.** 1985. Isolation of herpes simplex virus regulatory protein ICP4 as a homodimeric complex. J. Virol. **55:**329–337.
35. **Middleton, M. H., G. R. Reyes, D. M. Ciufo, A. Buchan, J. C. M. Macnab, and G. S. Hayward.** 1982. Expression of cloned herpesvirus genes. I. Detection of nuclear antigens from herpes simplex virus type 2 inverted repeat regions in transfected mouse cells. J. Virol. **43:**1091–1101.
36. **Mikaelian, I., E. Drouet, V. Marechal, G. Denoyel, J.-C. Nicolas, and A. Sergeant.** 1993. The DNA-binding domain of two bZIP transcription factors, the Epstein-Barr virus switch gene product EB1 and Jun, is a bipartite nuclear targeting sequence. J. Virol. **67:**734–742.

36a. **Mullen, M.-A., D. C. Ciufo, S. Gerstberger, and G. S. Hayward.** Unpublished data.

37. **Muller, M. T.** 1987. Binding of the herpes simplex virus immediate-early gene product ICP4 to its own transcription start site. J. Virol. **61:**858–865.
38. **O'Hare, P., and G. S. Hayward.** 1985. Evidence for a direct role for both the 175,000- and 110,000-molecular-weight immediate-early proteins of herpes simplex virus in the transactivation of delayed early promoters. J. Virol. **53:**751–760.
39. **O'Hare, P., and G. S. Hayward.** 1985. Three *trans*-acting regulatory proteins of herpes simplex virus modulate immediate-early gene expression in a pathway involving positive and negative feedback regulation. J. Virol. **56:**723–733.
40. **O'Hare, P., and G. S. Hayward.** 1987. Comparison of upstream sequence requirements for positive and negative regulation of a herpes simplex virus immediate-early gene by three virus-encoded *trans*-acting factors. J. Virol. **61:**190–199.
41. **O'Hare, P., J. D. Mosca, and G. S. Hayward.** 1986. Multiple trans-activating proteins of herpes simplex virus that have different target promoter specificities and exhibit both positive and negative regulatory functions. Cancer Cells **4:**175–188.
42. **Paterson, T., and R. D. Everett.** 1988. The regions of the herpes simplex virus type 1 immediate early protein Vmw175 required for site specific DNA binding closely correspond to those involved in transcriptional regulation. Nucleic Acids Res. **16:**11005–11025.
43. **Perry, L. J., F. J. Rixon, R. D. Everett, M. C. Frame, and D. J. McGeoch.** 1986. Characterization of the IE110 gene of herpes simplex virus type 1. J. Gen. Virol. **67:**2365–2380.
44. **Persson, R. H., S. Bacchetti, and J. R. Smiley.** 1985. Cells that constitutively express the herpes simplex virus immediate-early protein ICP4 allow efficient activation of viral delayed-early genes in *trans*. J. Virol. **54:**414–421.
45. **Pizzorno, M. C., M.-A. Mullen, Y.-N. Chang, and G. S. Hayward.** 1991. The functionally active IE2 immediate-early regulatory protein of human cytomegalovirus is an 80-kilodalton polypeptide that contains two distinct activator domains and a duplicated nuclear localization signal. J. Virol. **65:**3839–3852.
46. **Quinlan, M. P., and D. M. Knipe.** 1985. Stimulation of expression of a herpes simplex virus DNA-binding protein by two viral functions. Mol. Cell. Biol. **5:**957–963.
47. **Rihs, H.-P., D. A. Jans, H. Fan, and R. Peters.** 1991. The rate of nuclear cytoplasmic protein transport is determined by the casein kinase II site flanking the nuclear localization sequence of the SV40 T-antigen. EMBO J. **10:**633–639.
48. **Roberts, M. S., A. Boundy, P. O'Hare, M. C. Pizzorno, D. M. Ciufo, and G. S. Hayward.** 1988. Direct correlation between a negative autoregulatory response element at the cap site of the herpes simplex virus type 1 IE175 (α4) promoter and a specific binding site for the IE175 (ICP4) protein. J. Virol. **62:**4307–4320.
49. **Russell, J., N. D. Stow, E. C. Stow, and C. M. Preston.** 1987. Herpes simplex virus genes involved in latency in vitro. J. Gen. Virol. **68:**3009–3018.
50. **Sacks, W. R., C. C. Green, D. P. Aschaan, and P. A. Schaffer.** 1985. Herpes simplex virus type 1 ICP27 is an essential regulatory protein. J. Virol. **55:**796–805.
51. **Sacks, W. R., and P. A. Schaffer.** 1987. Deletion mutants in the gene encoding the herpes simplex virus type 1 immediate-early protein ICP0 exhibit impaired growth in cell culture. J. Virol. **61:**829–839.

51a. **Sha, L., P. O'Hare, and G. S. Hayward.** Unpublished data.

52. **Showalter, S. D., M. Zweig, and B. Hampar.** 1981. Monoclonal antibodies to herpes simplex virus type 1 proteins, including the immediate-early protein ICP4. Infect. Immun. **34:**684–692.
53. **Stow, N. D., and E. C. Stow.** 1986. Isolation and characterization of a herpes simplex virus type 1 mutant containing a deletion within the gene encoding the immediate-early polypeptide Vmw110. J. Gen. Virol. **67:**2571–2585.
54. **Watson, R. J., and J. B. Clements.** 1980. A herpes simplex virus type 1 function continuously required for early and late virus RNA synthesis. Nature (London) **285:**329–330.
55. **Yao, F., and R. J. Courtney.** 1992. Association of ICP0 but not ICP27 with purified virions of herpes simplex virus type 1. J. Virol. **66:**2709–2716.
56. **Zhu, X., J. Chen, and S. Silverstein.** 1991. Isolation and characterization of a functional cDNA encoding ICP0 from herpes simplex virus type 1. J. Virol. **65:**957–960.
57. **Zhu, X., J. Chen, C. S. H. Young, and S. Silverstein.** 1990. Reactivation of latent herpes simplex virus by adenovirus recombinants encoding mutant IE-0 gene products. J. Virol. **64:**4489–4498.
58. **Zhu, X., A. G. Papavassiliou, H. G. Stunnenburg, and S. Silverstein.** 1991. Transactivation by herpes simplex virus proteins ICP4 and ICP0 in vaccinia virus infected cells. Virology **184:**67–78.
59. **Zhu, X., C. S. H. Young, and S. Silverstein.** 1988. Adenovirus vector expressing functional herpes simplex virus ICP0. J. Virol. **62:**4544–4553.